LOW COST SOLAR POWER SYSTEM WITH OPEN LOOP TRACKING FOR RURAL AND DEVELOPING AREAS

LOW COST SOLAR POWER SYSTEM WITH OPEN LOOP TRACKING FOR RURAL AND DEVELOPING AREAS

A Thesis Presented to

The Graduate School of Bangkok University

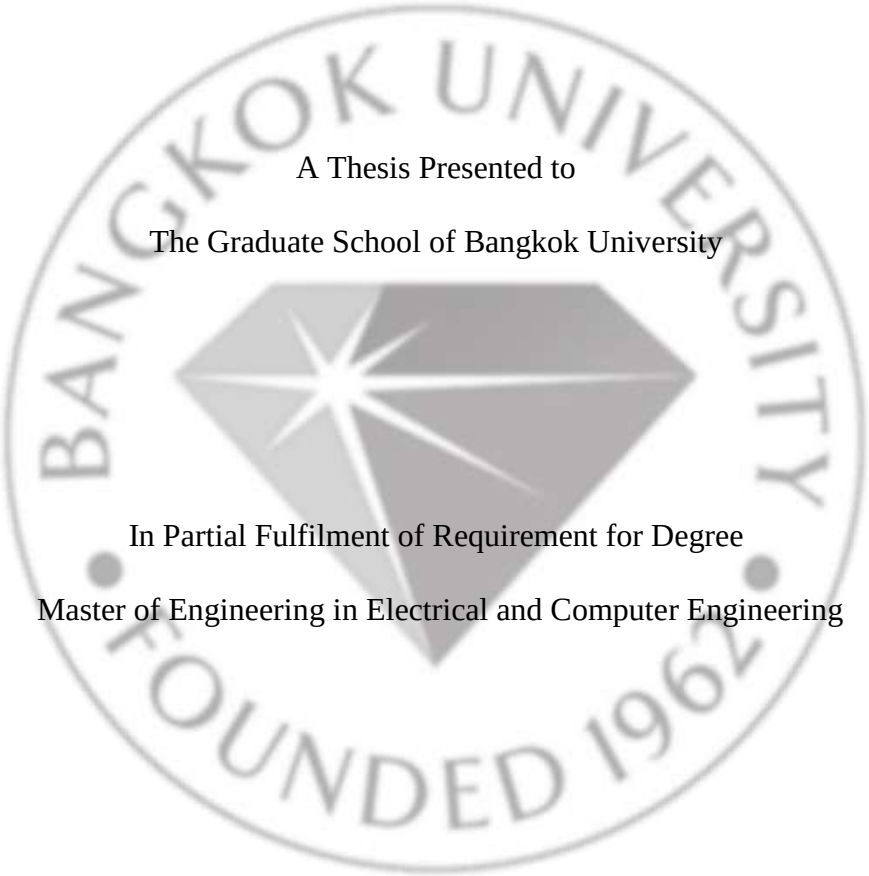

In Partial Fulfilment of Requirement for Degree

Master of Engineering in Electrical and Computer Engineering

by

Eidi Mohammad Atif

2020

This thesis has been approved by

School of Engineering

Bangkok University

Title : LOW COST SOLAR POWER SYSTEM WITH OPEN LOOP TRACKING FOR RURAL AND DEVELOPING AREAS

Author : Eidi Mohammad Atif

Thesis Committee :

Thesis Advisor

(Dr. Waleed Mohammed)

Thesis Co-advisor

(Dr. Karel Sterckx)

Graduate Program Director

(Asst.Prof.Dr. Chakkaphong Suthaputchakun)

External Representative

(Dr. Tanujjal Bor)

(Asst.Prof.Dr. Wisarn Patchoo)

Dean of the School of Engineering

21 / 05 / 20

Atif, E, M., Master of Engineering and in Electrical and Computer Science, March 2020, Graduate School, Bangkok University.

Low Cost Solar Power System with Open Loop Tracking for Rural and Developing Areas (66 Pp)

Advisor of Thesis: Waleed S. Mohammad, Ph.D.

ABSTRACT

Solar energy continues to enjoy interest and is becoming one of the important elements in the world's future energy consumption and economic growth. One way to increase the use of solar power systems, particularly in rural and developing areas, is through the employment of low cost, power efficient systems. This paper presents a possible low cost solution where an open loop tracking system is implemented with a small size 50 Watt Monocrystalline Photovoltaic (PV) panel. The system's performance is monitored at different tropical weather conditions. In addition, the output power is measured and compared between a static solar panel and one that includes the proposed tracking system. The measurements over the course of five months in Pathum Thani, north of Bangkok (Thailand), showed that the output energy with tracking system, on average, is 12 % higher than with static panel (45 Watt hour (Wh) compared to 36.5 Wh). The overall generated energy in 7 hours in a day are 315Watt hour per day (Wh/day) and 255 Wh/day for tracking and static panel respectively. On rainy days, the average measured output power is reduced to 25% of that on the sunny days. The experimental results have been compared to those of a deduced first order simulation output and this over a period of five months. The experiment shows similarity in the trend between experimental and simulation results.

Finally, multiple sensors were added to the solar unit, and measured environmental data sent obtained by these sensors were over a low bandwidth communication link, and recorded/processed on a remote server.

ACKNOWLEDGEMENT

I am greatly indebted to my parents who have deepest guidance, love, support and motivation during my whole life. They have always encouraged me to continue and overcome difficulties all times. It is impossible for me to realize my goals without them. I appreciate my wife Marzia Khalil for her understanding and love during the past few years. Her supports and encouragement were in the end what made this dissertation possible.

I would like to express my special appreciation and thankful to my advisors Dr. Waleed S. Mohammed and Dr. Karel Sterckx for their help and support during the course of my study. I wish to express my profound gratitude to all Bangkok University Center of Research in Optoelectronics Communication Control (BU-CROCCS) members for their excellent suggestions and encouragement, which were useful for my research. Also, I would like to thanks Dr. Ian Grout from the University of Limerick for his help in my system during his visit to Bangkok University.

It would be great to thank the BUTA scholarship, and Bangkok University's School of Engineering for providing me with a scholarship and providing facilities and opportunities to conduct my master's research.

TABLE OF CONTENTS

Page

Page

Page

LIST OF TABLES

Page

LIST OF FIGURES

Page

ACRONYMS

BLE	Bluetooth Low Energy
E	East
N	North
PCS	Personal Communication services
PV	Photovoltaic
WSN	Wireless Sensors Network
ISM	Industrial Scientific and Medical
TW	Tera Watt
OLSTS	Open Loop Solar Tracking System
GPS	Global Positioning System
HART	Highway Addressable Remote Transduce
LPWAN	low Power Wide Area Network
IoT	Internet of Things
WPAN	Wireless Personal Area Network
NB-IoT	Narrow Band Internet of Things
PLC	Programmable Logic Controller
LR-WPAN	Low Rate Wireless Personal Area Network
HART	Highway Addressable Remote transducer
WSN	Wireless Sensor Network
CSS	Chirp Spread Spectrum
ISM	Industrial Scientific and Medical
GSM	Global System for Mobile communication
LDR	Light Depended Resister

OPSTS	Open-Loop Solar Tracking System
PWM	Pulse Width Modulation
AC	Alternating Current
DC	Direction Current
USB	Universal Serial Bus
ISP	Internet Service Provider
SCC	Solar Charge Controller
PWMSCC	Pulse Width Modulation Solar Charge Controller
MPPTSCC	Maximum Power Point Trackers Solar Charge Controller
SRAM	Static Random Access Memory
EEPROM	Electrical Erasable Programmable Read-only memory

CHAPTER 1

INTRODUCTION

1.1 Background

Energy is one of the most important elements in modern life, which is increasingly demanded all around the globe. It is almost impossible to access sustainable development without the influence of energy resources (Ralph & Hans, 2003). A survey was performed in 2014 to estimate the power supplied from different sources around the globe. The results indicated that coal produces 40.8%, natural gas and oil 25.9%, hydro power 16.4%, nuclear 10.6% and renewable energy produces 6.3% (Mohammad & Amith, 2019). Fossil fuel resources (e.g. coal, oil and natural gas) are limited while they provide more than 65% of global energy consumption. The risk of running out of these resources, especially with the increasing energy demand due to constant population growth and rapid technology development, brings a strong need for alternative resources. Moreover, the global warming and air pollution are critical issues that the world is facing (Karmaker & Rahamn, 2019) Therefore, researchers are pushing towards finding a sustainable replacement for fossil fuel. Renewable energy is a strong candidate to provide a valid solution to the needed energy supply all over the world (Christopher & Thomas). One of the most promising renewable energy sources is solar power. Photovoltaic systems can replace conventional energy compared to other renewable sources (Solaun & Cerdá, 2019). Solar power is a free resource which is accessible everywhere the sun light is received. The solar cell directly or indirectly converts light intensity into electrical

current. It was estimated that covering 0.16% area of the earth with 10% conversion efficiency solar panel can provide nearly double the world consumption rate of fossil fuel energy (Carballo & Bonilla, 2018).

In general, solar energy efficiency is based on three factors: nature of the silicon crystal (single or multiple) that the solar panel is made of, energy convertor efficiency, and amount of solar radiation that falls onto the PV-panel (Ferdaus & Mohammed, 2014). Solar light intensity is maximized when the panel is normal to the sun direction, which requires a tracking mechanism as the earth moves around its orbit in a complex motion (Hou & Wang, 2010). This motion includes daily and seasonal movements (Tarujyoti, 2012). The daily movement causes the sun to move from east to west direction, while the seasonal motion causes a tilt from south to north and vice versa (Tarujyoti, 2012). Therefore, to keep PV-panel parallel toward the sun surface it is necessity to consider the sun position in two angles: azimuth (tracking the sun position in daily motion) and evaluation (tracking the sun position in seasonal motion) (Singh & Kumar, 2018).

Commonly, there are two important types of solar tracking controlling systems to keep the PV-panel surface parallel toward the sun direction [(Ferdaus & Mohammed, 2014), (Lee, & Chou, 2009)]: close-loop (feedback) control solar tracking mode and open-loop tracking system. Close-loop tracking uses one, or two light sensors to detect the solar position in near real-time fashion. It gives feedback to the controller to arrange the PV-panel position for the highest light intensity in order to maximize the energy generated by the panel (Lee, & Chou, 2009). Although the close–loop tracking provides high accuracy, the system can be affected by the weather

condition, especially in cloudy time which can causes tracking errors. The closed-loop module can as well be costly (Mohammad & Amith, 2019).

In contrast to close-loop, open-loop solar tracking system (OLSTS) uses microcontroller programmed with pre-calculated sun location. An efficient mechanism to perform solar tracking with low-speed and minimum motors power consumption can be as well implemented [(Gerro & Robert, 2015), (Same, & Srpcic, 2017)]. The sun vector describes the sun azimuth and elevation angles from the perspective of a specific Global Positioning System (GPS) orientation on the earth with a real-time. In this system, the tracker can be implemented using common microcontroller such as Arduino (Aigboviosa & Anthony, 2018). Moreover, OLSTS is able to track the sun location and maximize the output energy on both sunny and cloudy times. The major drawback of OLSTS is the sole dependency on astronomical parameters with no feedback for error correction (Huynh & Nguyen, 2013).

In most developing countries especially in rural areas, many people do not have access to electricity to light their homes, and irrigate their farms (Wazed,& Hughes, 2017). Therefore, mounting a small solar power station in every family's household can provide their basic energy necessity as a sustainable and permanent source (Ershad, 2017).

In this work, an OLSTS is implemented using low power motors to design and construct a simple dual-axis solar tracker. Tracking is done through pre-calculated sun orientation based on the geographical location, time and date. A Real time clock is used to get the time and date. Though the developed system includes a light intensity sensor, it does not use it for tracking. The light sensors are used mainly to monitor the environment and indicate different weather conditions in combination with humidity

and temperature sensors. The study focuses on minimizing the motor operation time keeping high amount of energy absorption. This is to ensure the enhancement of the output power in the tracking system compared to the static case. Additionally, the target of this study is to serve regions with continuous electricity shortage problems particularly in Afghanistan and Thailand. As Thailand is located in 15.870º N 100.995º E, the average annual solar radiation is 5. 06 kWh/m^2.day for 2643 hours of sun in a year (Arunpold & Tripathi, 2014). Afghanistan is located 35.14º N, 76.7100 º E. The annual solar radiation is 5kWh/m^2day for 3000 sunny hours/year in Afghanistan (Raheleh, & Meysam, 2017). Furthermore, both countries have suitable conditions to use solar energy as the main source of power supplying the rural areas particularly for home lighting, irrigation, and environment monitoring.

It is worth mentioning that the main contribution this work presents is a possible low cost solution based on open source technology and commonly available Arduino platform. The demonstrated platform targets regions of urgent need to life basics such as lighting and providing environment monitoring capabilities. In addition, the proposed tracking system can be mainly useful in rural areas which are located far from the equator. For example, in Afghanistan the sun radiation makes 32° angle to horizontal on 21th December and the winter days are short. Thus, using a tracking system is more beneficial than a static panel.

One important factor in environment monitoring is the need for remote data collection. Wireless sensor network have been implemented in several research in different areas such as industrial controlling, infrastructure, agricultural monitoring, and surveillance (Bhuvaneswari & Balakumar, 2009) Wireless sensors node applies power-limited battery as energy supply, there are large number of nodes extensively

wide and complex environment. It is very difficult to replace the wireless sensor network battery (Bhuvaneswari & Balakumar, 2009). This study focus to distribute solar power to supply wireless sensors network for the field application. Several sensors are added to the solar panel to observe ambient temperature, humidity, light intensity as well as the produced current and voltage. These data are transmitted over narrow band communication and recorded in a remote server for data analysis. Another strategy that the research attempted to reduce power consumption, which low power consumption devices selected and created a sleep mode operating system (Selvakumar, 16).

1.2 Objectives

The principle targets of this research are listed as follows.

i) Maximization of Solar cell output power by considering tracking sun trajectory in the sky.
   - Implementation of open-loop tracking system

ii) Demonstration of solar powered multiple sensors unit at the for field application.

iii) Minimization of power consumption by the unit.
   - Optimization of controllers sleep mode

iv) Selection of the wireless communication module.

v) Demonstration of environment monitoring system.
   - Installing wireless sensor node with multiple sensors by Arduino microcontroller.
   - Connecting the node to the internet.

1.3 Problem statement

As mentioned in section 1.1, sustaining the current energy resources is a serious challenge around the world. This issue is more severe in developing countries particularly in the rural areas. In such regions many people may not have access to electricity for lighting their home. Hence, a solar unit that can provide basic energy resource for regions in need with environment monitoring capabilities can be of great help. The energy consumption of hardware devices on a continuously operating unit should be minimized. This is such that the excess energy can be utilized in household lighting and charging electronic devices. The challenge is to keep the node at low cost, minimum complexity and efficient energy generation.

1.4 Scope and limitation

The research relies on theoretical studies, simulation, programming, designing, and building the mechanical solar tracker structure. The study aims to demonstrate a small solar power plant that can be used in rural areas. The tracking system is based on OLSTS, which is programmed on real-time control. The research limitation includes PV-panel output power simulation, electrical circuit simulation, controlling part programming, data transmitting section programming, and solar power plant system designing.

1.5 Thesis Outline

This thesis starts in chapter one with a general background of solar energy harvesting and environmental monitoring. This illustrates the main motivation of the research. In chapter two, solar tracking system and wireless communication devices, basic background information as well as related works are presented. Chapter three

introduces the system model, the simulation approach, the system design and its structure. It as well illustrates the electrical circuit design and programming include tools. Chapter four discusses the evaluation of the solar tracking system implantation. That includes misfit angle description, the tracking system energy consumption and the effect of temperature on solar panel output voltage. Data analysis according to both solar tracking system and static panel in different weather conditions are presented and the result compared with simulation output power.

CHAPTER 2

LITERATURE REVIEW

This chapter summarizes several research papers related to this study. The literature review presents the already existing work on theoretical analysis of the sun trajectory, solar panel tracking system implementation, programmable logic controller (PLC) hardware devices.

2.1 Solar radiation

The sun radiates energy in the form of electromagnetic energy. The amount of energy that reaches the earth from the sun is referred to as solar radiation. This is used to define the amount of solar energy per unit square area reached over a given time period (John & William, 2013). The solar radiation that reaches the earth can be assumed to be a collection of rays that diffuse through the atmosphere and reflect from the ground. The amount of rays reaching onto a solar panel depends on the clarity of the atmosphere (John & William, 2013). The angular direction of the solar radiation depends on the target location on earth and the different time and date along the year. That affects the output efficiency of the each solar cell and hence the panel in total. To improve the efficiency of the panel yield, one requires a relatively accurate sun tracking mechanism, which is called solar tracking system (Weller & Hemmerle, 2012).

2.2 Sun trajectory

It is a fact that the earth travels around the sun once a year and rotates daily around its own polar axis. Therefore, it is important for any solar taking system to be

able to determine the mathematical trajectory; the respective change of the sun position in both hourly and seasonal visible from the earth (Lee & Huang, 2013). The sun position at a given time varies in different season or every month [(Sierke & Kusakana, 2017), (Tarng & Ou, 2018)]. Figure 2.2.1 illustrates the sun trajectory during different seasons of the year.

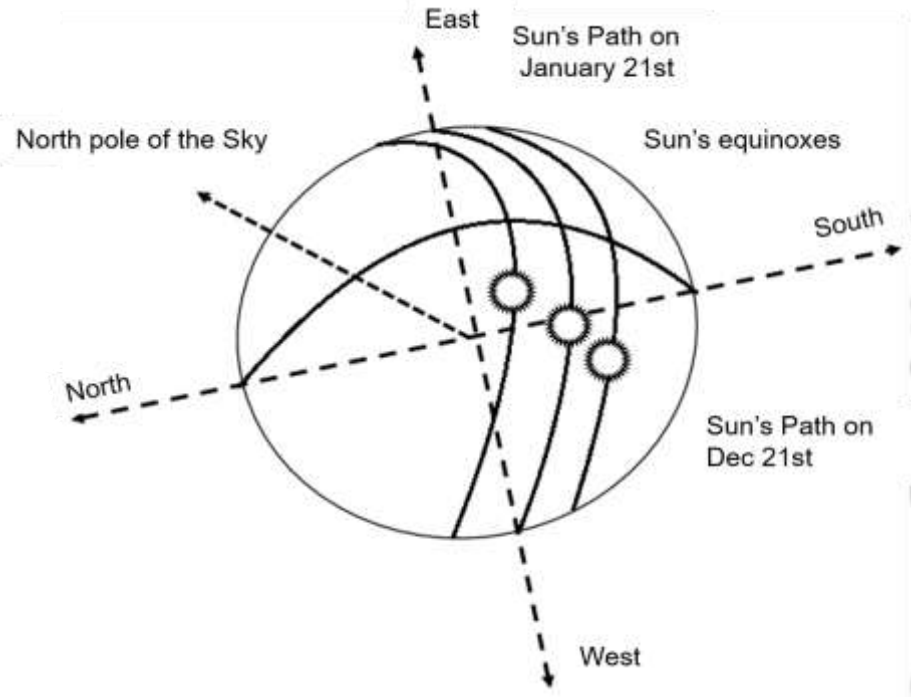

Figure 2.2-1: Sun path during different seasons of the year

In the solar tracking system, it is important to determine the various angles that the sun's daily motion and seasonal change make on a specific location of the earth (Guala & Mansourian, 2015). The study in (Guala & Mansourian, 2015) considered the solar radiation angles calculations based on the altitude, surface azimuthal angle, slope angle hour angle and the solar azimuthal angle. Solar altitude is the angle between the horizontal plane and the declination angle that shows the sun position at noon (i.e., when the sun is on the local meridian). In the case of the

equator, the altitude is between (-23.45º and +23.45°), (Gerro & Robert, 2015). Slope angle is the angle that the solar panel surface makes on horizontal. Surface azimuth angle is the deflection of the projection on a horizontal plane of the normal to the surface from local meridian. The south has zero azimuthal angle. The west has positive angles and the east has negative values. The surface azimuth angle is between -180° and +180° (Singh & Kumar, 2018). The hour angle is the sun replacement angular from east or west of the local meridian due to rotation of the earth on its axis. It is determined as 15°per hour (Department of Agricultural West Australia, 2004). Due to the sun displacement, hour angle is negative in the morning and positive in the afternoon. The zenith angle is measured between the line from the sun and the vertical vector that makes the zenith angle, which is the angle of incidence of the beam radiation on a horizontal surface (Chin & Babu, 2011). Finally, the solar azimuth angle is the replacement angular from south of the projection of the light radiation on the horizontal plane.

2.3 Types of solar tracking system

Figure 2.3-1 shows that the sun position makes different angles at any point on earth. Thus, it is necessary to determine different types of solar tracking system according to the sun position. One-axis sun-tracking design is shown in Figure 2.3.1. This includes a vertical-axis tracker which is collinear with the zenith axis. The tilted axis tracker is also known as the zenith sun tracker. In this configuration, the tracking axis is tilted from the horizon by an angle oriented along the north-south direction (e.g. Latitude-tilted-axis sun tracker). In the horizontal-axis tracker, the tracking axis remains parallel to the surface of earth and it is rotates along East-West

(Sadeq, 2017). In the two-axis sun tracking system the tracker follows the sun in the horizontal and the vertical planes. In this case the solar collector must be free to rotate about the azimuth and the elevation axes. The tracking angle about the azimuth axis is the solar azimuth angle, and the tracking angle about the elevation axis is the solar elevation angle. The dual-axis system tracks the sun such that the sun vector is always normal to the aperture as to attain nearly 100% energy collection efficiency (Jumaat & Azlan, 2018).

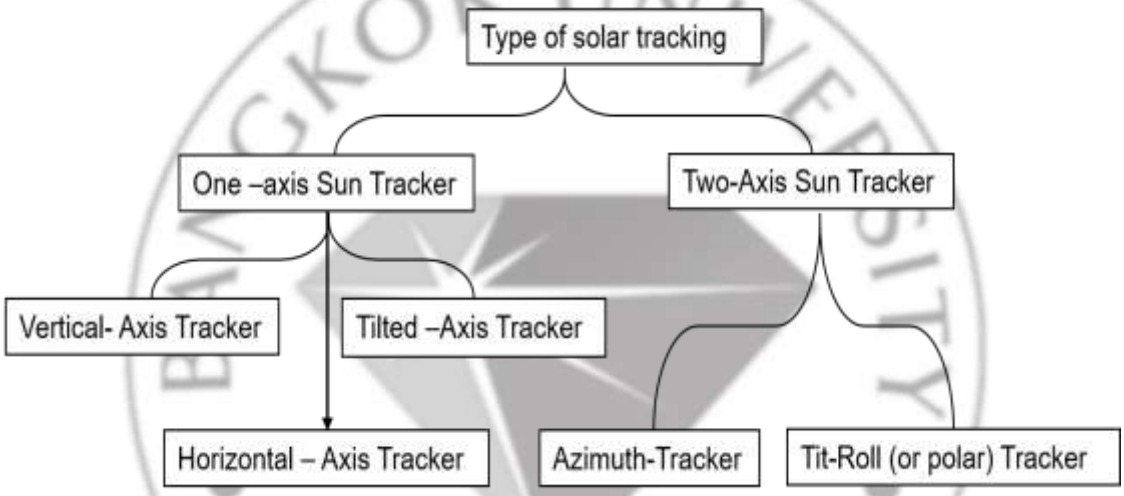

Figure 2.3-1: Type of solar tracking system

In literature, a single axis solar tracking system was designed and installed to rotate the solar panel from east to west using one sensor to give a feedback to the controller unit (Chin & Babu, 2011). In the system, two gears were implemented to hold the panel and one motor was mounted to run the tracker on a single-axis. In another implementation, a horizontal single-axis solar tracker was designed using Arduino as a microcontroller unit (Sirigauri & Raghav, 2015). In that system, light sensor and liquid crystal display (LCD) were utilized for giving the feedback. One servo motor was installed for rotating the solar panel, and a light-dependent resister

which was programmed on a reset off/on button. The system was tracking the sun daily motions from east to west. A small dual-axis solar tracking system was designed using two servo motors for panel rotation and two light depended resisters (LDR) for feedback (Sirigauri & Raghav, 2015). The servo motors follow the sun position on daily and seasonal movements depending on the sun position. This is achieved through an Arduino unit that receives the signal from the LDRs. It then send commands to the motors' drivers to keep the panel parallel towards the sun. In addition, 9V battery was mounted in the system to supply the microcontroller unit. In another work, a hybrid dual-axis solar tracker was designed using one motor for daily motion tracking based on the feedback from a light sensor implemented in the system Ferdaus & Mohammed, 2014). The motor controller continually operates during the day. Another motor was mounted and programmed to move a few times over the year to track the sun position from north to south and vice versa. A lower cost close loop solar tracking system was designed using one axis tracker with optical sensor. The second axis was programmed with real-time clock to calculate the sun location and control the motors using Arduino board as controller unit of both axes (Chong &Wong, 2011). Similarly, one closed-loop solar tracking system was demonstrated using two optical sensors to indicate the position of the solar image on the receiver. These sensors generate feedback signal to the microcontroller and the trackers receives an order from the microcontroller to run or stop (Prajapati & Patel, 2015).

In literature, there exists a few research works which deal with open-loop solar tracking system (OLSTS) implementations. As a dual-axis OLSTS was designed using a computer unit, data acquisition card, relays, lead-acid battery, and motors

(Melo & Filho, 2017). The system updates the time, date and geographical location and calculates the needed solar angles, which are then used to rotate the panel accordingly. A single-axis OLSTS was designed that is driven by permanent magnet direct current motor through a linear actuator. The linear actuator converts the rotational motion into linear motion and then operate the metallic surface on which the panels are mounted (ÖZturk & Alkan, 2016). An OLSTS was designed and mounted using two DC-motors. One DC-motor was joined to rotate to control the tilt axis and the other controlled azimuth axis (Kevrak & Gunduzal, 2010). Two motorized satellite dish antenna devices was used as actuators, as one of the dish antenna was fixed and the second was mounted on fixed apparatus to move on tow axes. In addition two linear potentiometer were mounted on the other side of the shafts to read the sun position in degree.

In literature, there exist common wireless communication devices that are widely used in different field applications and environment monitoring such as Bluetooth, LoRa, ZigBee, NB-IoT, SigFox, HART and Z-wave. Bluetooth technology was introduced by IEEE working group 802.15.1 in 1999 (Dahiya, 2017). Later it was developed to a high-speed Bluetooth 4.0 low energy (BLE) (Joshua & Matthew, 2015). Bluetooth low energy was designed and approved by wireless personal area network WPAN by IEEE (802.15.3) in hardware, software, sensors. BLE is a common wireless sensors network that widely used in different aim around the world, but it has a short range of operation. ZigBee was then introduced as a smart low power consumption, low-cost and low data rate (250kbps) wireless personal area networks [(Garcia & Barreiro, 2008)]. This module is a medium access control

(MAC) layer that was built by IEEE 802.15.4 standard. It is used in different areas for multiple aims such as home controlling, industrial, and health care. This module is used in both network and application layers. Both Bluetooth and ZigBee are short range technologies. Low power wide area network (LPWAN) was then demonstrated for long range communication (Kabalci & Ali, 2019). The module is increasingly getting popular because of its long range, low power and low cost. LPWAN can cover ranges up to 10 to 40 km in the rural area (without obstacles) and one to five km in the urban zone. There are three types of LPWA: long range (LoRa), narrow band internet of things (BN-IoT) and (SigFox). LoRa communication protocol is a radio frequency method technology that modulates in sub-GHz ISM band, which is used for wide area network application (Zhou & Zheng, 2019). This module is a bidirectional communication that was provided by chirp spread spectrum (CSS) technology, which diffuse narrow-bands signal around 5km in urban zone and over than 20 km in rural zone. LoRa has three bandwidth classes for communication: 125, 250, and 500 KHz. The module transmission power is limited between 2 to 20dBm in different regions of the world. NB-IoT technology is specified in destitution 13 of 3GPP in 2016 (Nikoukar & Raza, 2018). NB-IoT is able to coexist with global system for mobile communication (GSM), and long-term evolution (LTE). It uses licensed frequency bands between (700 MHz, 800 MHz, and 900 MHz). NB-IoT maximum payload length range is 1 km in the urban and 10 km in the rural areas. The last type of LPWAN is SigFox. It is an unlicensed ISM narrow band, which is used for complex bands (for instance: 868 MHz in Europe, 915MHz in North America, and 433MHz in Asia) (Rubio & Cerdan, 2019). By adding an ultra-narrow band, the module changes to a frequency bandwidth efficiency scheme with very low noise

level, low power consumption, and high receiver sensitivity. SigFox was designed in low cost antenna with maximum transmit of 100bps. At first SigFox, was supported as uplink communication, that the maximum payload length for each uplink message was 12bps. The module was supported with bidirectional downlink communication technology. Downlink communication is a narrow band long length wireless communication that can cover 10 km length in the urban zone and 40km in the rural area with sending maximum message of 8 bps.

In literature, to decrease hardware devices energy consumption, this study considered sleep mode creations in operation system. Such, ZT-10 active tag is a ISM band with remote wakeups used to support IEEE 802.15.4, which the ZT-10 tag operate at the 2.4 GHz. The ZT-10 tag apply a range up to 70 m for bidirectional communication. At the idle situation, the ZT-10 tag current decrease to 2μA, which several orders of magnitude lower than typical 802.15.4 radios. In the result, the tag can remain in ide mode all the time until it receives a wake up signal from a remote sender (Jurdak, Antonio, 2010).

CHAPTER 3

METHODOLOGY

This chapter presents the solar tracker implementation, the efficiency and drawback of the tracking system. It explains the research procedure used to carry out the research objective in order to simplify the design process. The chapter is divided into three different parts: simulation, designing a small solar power plant, which is based open loop solar tracking system, and programming controlling and wireless sensors network communication. Figure 3-1 illustrates the implementation of the system including data collection and analyses.

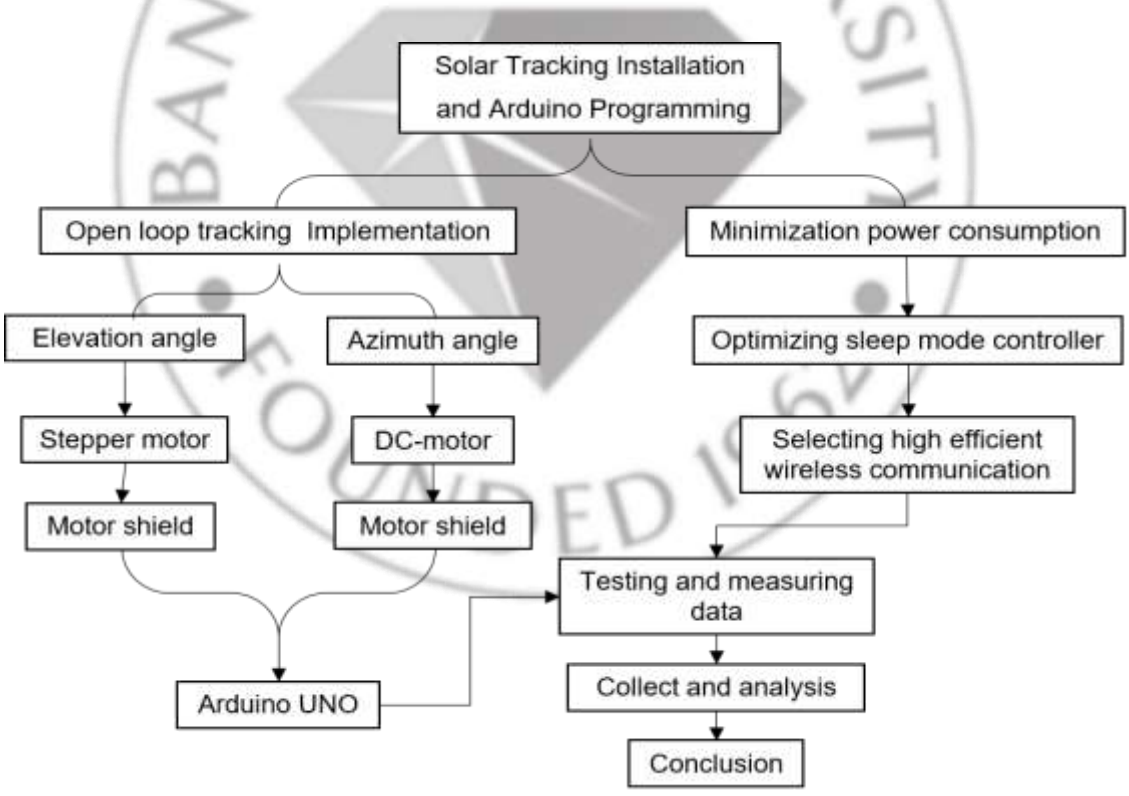

Figure2.3-1: Implementation frame work of the thesis

3.1 Solar energy estimating

Different research results show that a unit square meter of the sun surface releases amount 1322 to 1395W/m^2 energy. Around 25-30 % of the solar radiation is lost in the atmosphere and 70-75% reaches the earth surface Therefore, in equation 3.1, 1000 W/m^2 solar energy is considered to reach the earth surface. But the amount of reached energy estimate in consider to solar radiation angles from a specific position of the earth which the result may be different on different region of the earth.

Based on Stefan-Boltzmann law (John & Beckman, 2013) the sun can be assumed as a blackbody. Accordingly, the amount of solar energy reaches one square meter of earth's atmosphere can be calculated following the model in figure 3.1.1 as follows.

$$E_{sun} = \frac{\sigma T^4 \times R^2}{D^2} = 1356 \frac{W}{m^2} \qquad 3.1$$

Where E_{sun} is amount of solar energy that reaches on square meter of earth, σ is the Stefan-Boltzmann constant that $\sigma = 5.6697 \times 10^{-8} \, W/_{m^2} \; k. \; T = 5777° \, K$ is the sun surface temperature. R is the sun radius, $R = \frac{D_{sun}}{2}$ and D is distance between sun and earth.

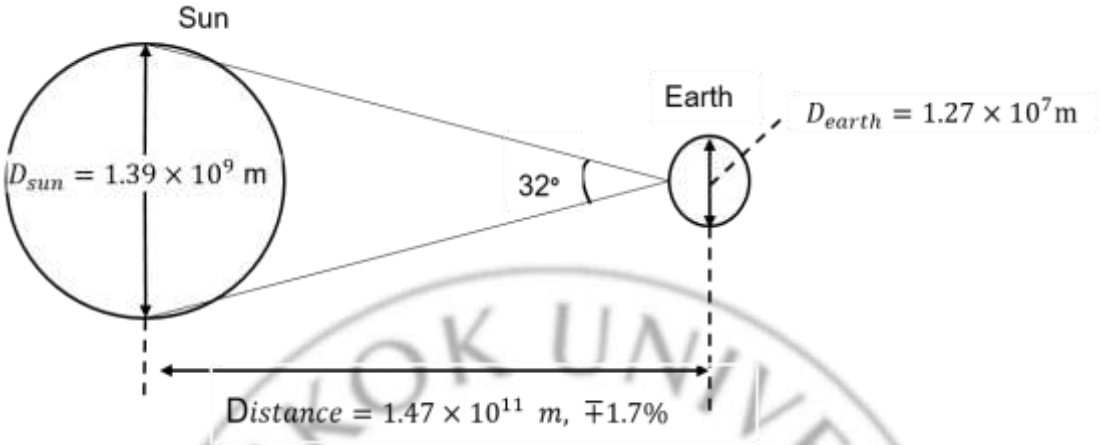

Figure 3.1-1: Relationship between sun and earth distance

Down going solar energy after atmosphere filtering is;

$$P_{Tot}(T) = E_{sun} \times \int_{\lambda_{min}}^{\lambda_{max}} \tau atmosphere(\lambda) \approx 1000 \frac{W}{m^2} \qquad 3.2$$

Where $\boldsymbol{\tau}$ is the atmosphere transmission, E_{sun} is passing light wavelength, and E_{sun} amount of solar energy on one meter square of earth.

The power irradiating the surface of the earth then fluctuates with the second power of sinusoidal function of the sun elevation angle. The amount of solar energy on a unit square meter area on earth during one day can be estimate by integrating over a given time.

$$E_{day} = \int_0^{nhr} \sin^2(\omega t) \times P_{Tot}(T) \qquad 3.3$$

Where, ω is the solar angle according to time. As the Earth rotates 360º around its axis within 24 hour, the sun angle can be determine by equation 3.4.

$$\omega = \frac{2\pi}{24hr} = \frac{\pi}{12} \times \frac{1}{hr} = \frac{15^o}{hr} \quad 3.4$$

3.2 Simulation of the system

The main purpose of the simulation part in this study is to estimate the output energy of a small solar power plant considering the location on earth using two axis solar tracking system. The solar panel conversion efficiency is calculated using PV- Syst software that is commonly used for renewable energy system simulation (Kandasamy & Prabu, 2013). The main limitation of this software is the minimal solar panel area of 2.2m^2. In the practical implementation of this study a 0.357 m^2 panel is used. Therefore, this study system the PV-System is used to simulate a 2.2 m^2 area PV-panel. The results are then scaled down to match the desired panel capacity.

3.3 Design and implementation

This work focuses to developing a simple, low cost, easy to build and efficient open loop solar tracking system with additional environmental monitoring capability. This suits the implementation in rural areas, devastated regions and places with frequent electricity outage. The tracking system can be easily built and programmed with low cost using equipment that can be available in the local market. The system is designed to minimize the operation power consumption. This is done by dividing the task into two parts: mechanical design and electrical circuit design.

3.4 Mechanical design

The demonstrated solar tracking system utilizes two motors for azimuth tracking (DC-motor for East–Waste motion), and elevation tracking (stepper motor

for North-South). The mechanical design and implementation is divided into three parts: panel carrier, panel carrier rotator and linear actuator as depicted in figure.

3.4.1 The panel carrier

The panel carrier comprises of an aluminum rectangular frame to support a 50 Watt PV-panel, a 3D-printed circular joint and a post. The 3D-printed joint is connected to the panel frame with two bearings to facilitate the elevation motion. The post is used to connect the solar panel to the rotator through a 3D-printed large gear (diameter = 144 mm and 150 teeth) mounted at the rear end of the post. The panel carrier rotator comprises of a small gear (diameter = 32 mm and 33 teeth) coupled to a DC-motor that is mounted to an aluminum base to support the azimuth rotation between (0^o,180^o). The large gear completes one complete cycle every 4.5 rounds of the small gear.

3.4.2 Panel Carrier rotter

It is used to hold the PV-Panel on the horizontal bases of 50 Watt panel, gear, bearing, screw, rectangular and circular Aluminums frame it carries the panel which both frames connect together by bearing screw. As the gear installed straight to frame and the motor rotate the panel on Azimuth axis between (0, 180) degrees, as the figure 3.4.1b determine the panel carrier rotator part.

3.4.3 The linear actuator

The linear actuator converts circular movement to linear vertical motion that ensures panel elevation to accommodate for the seasonal angle change of the sun. It

comprises of a threaded rod, a nut connected to the panel through a rod, bearings and screws. The threaded rod is directly connected to a stepper motor. Motor rotation, turns the rod causing the nut to move linearly up or down. The rod connected between the nut and the end of the panel causes the elevation motion as it is shown in Figure 3.4.1c.

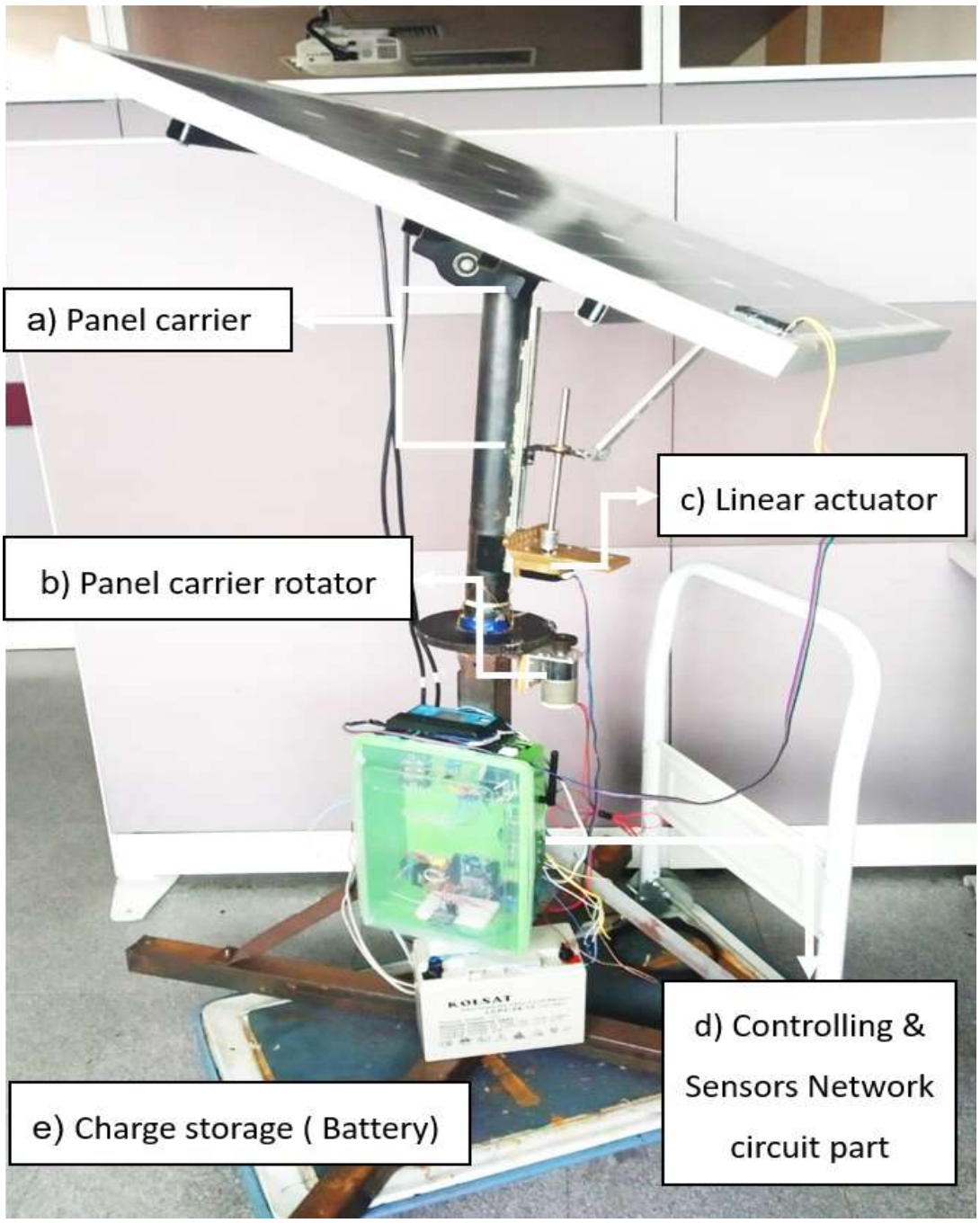

Figure 3.4-1: Structure of open loop tracking system

3.5 Electrical circuit design

This section is divided into two units: movement unit and controlling unit. In the movement unit, two 12V motors (stepper motor and DC-motor) are used. The Stepper motor moves the PV-panel on the vertical axis and DC-motor rotates the solar panel on the azimuth axis. Two motor drivers type (L298N) are installed in the controller unit. Both motor drivers include real time clock and they are programmed by Arduino UNO board to control the motion speed. The whole system powered by a (12 V) battery that is powered by the solar panel. The diagram for the electrical circuit design is shown in figure 3.5.1.

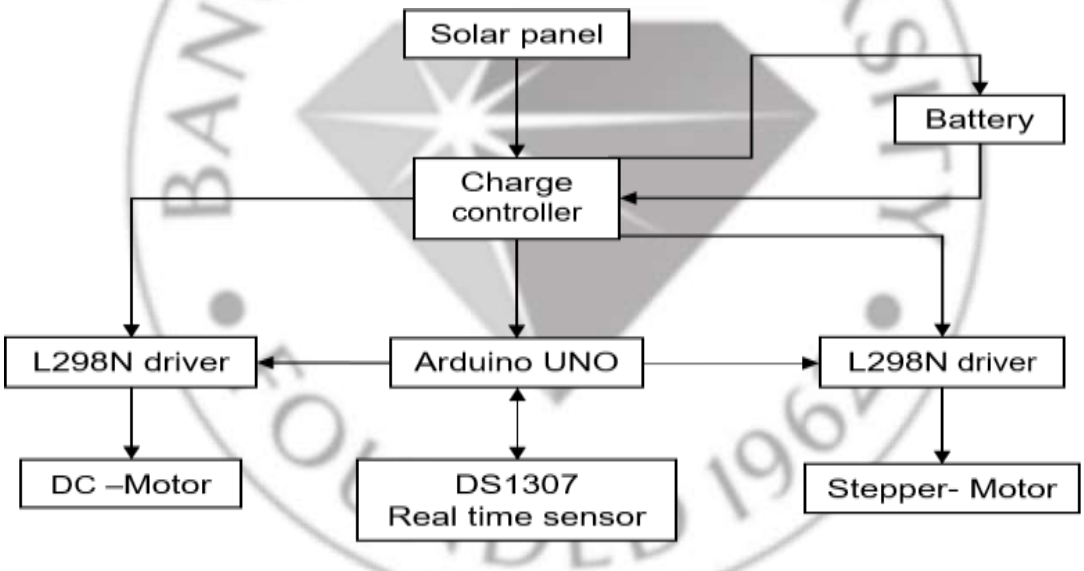

Figure 3.5-1: Electrical circuit design of solar tracker

3.6 Open loop tracking system

Figure 3.6.1 shows the dual axis open loop solar tracker system implementation mechanism based on real time clock. Bangkok University's main campus, where the experiments were conducted, is located at 13.986º N and 100.66º E. The whole system and the tracker controller are programmed using

Arduino considering local real time. The system is programmed such that the DC- motor rotates the system clockwise from east to west during the day to track the sun position. In the evening, the motor rotates back the system in anticlockwise direction to the initial position in one-step. The motor then enters a sleep mode during the night time. Since the location of the installed solar tracking system is close to the equator, tracking along the elevation–axis can be complex during the different seasons. For instance, the stepper motor that controls the elevation motion might need to rotate ones in a day in the period from 21th March to 21th September. However, one rotation every week can be sufficient in period from 21th September to 21th March.

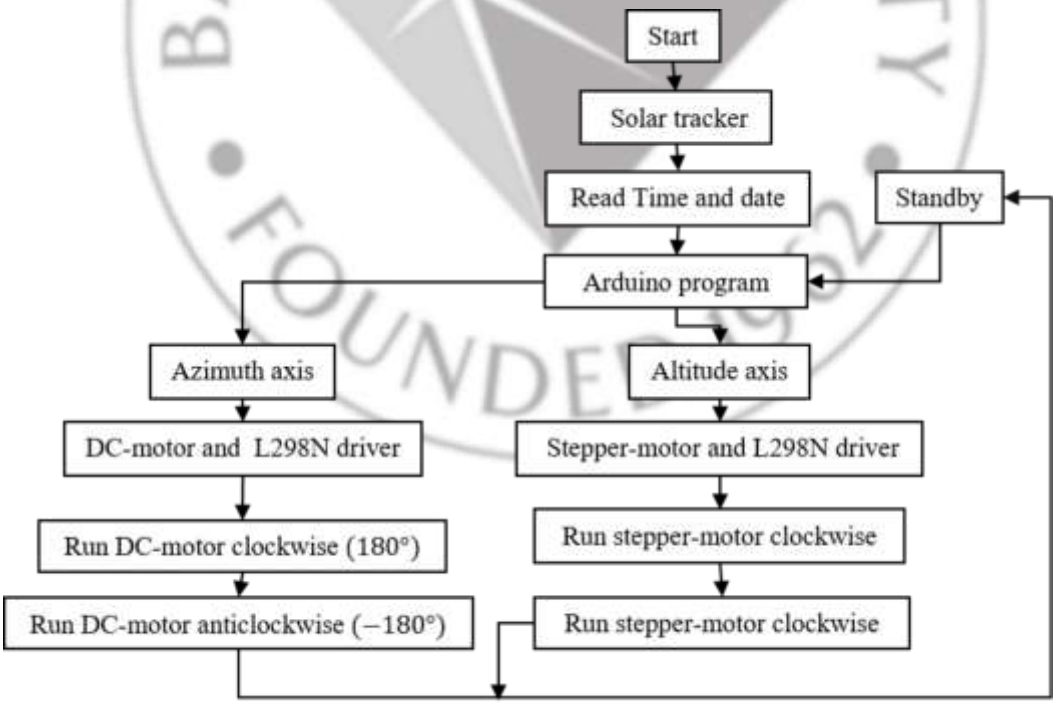

Figure 3.6-1: Bloch diagram of open loop solar tracking system

3.7 Sensor circuit design

In addition to its powering application, several sensors are added to the solar unit in order to monitor its performance as well as to sense environment conditions. The following sensors have been included:

The main focus of this work is the development of small solar power plant that can be implemented in rural areas with a capability of remote environment monitoring for applications such as smart farming (repetition of an earlier sentence). Remote monitoring requires a transmitter and a receiver antenna. Originally, two nRF14L01 units are used one for transmitting and one for receiving data. Hence, the nRF14L01 is a short range wireless communication of 100 meters maximum distance, it required a long range wireless communication devices to monitor the system far away. Therefore, it is worth mentioning that this study used a NB-IoT (Narrow Band Internet of Things) which is connected to AIS Magellan dashboard to send the sensors' data over the internet. The recorded data on AIS Magellan website are then requested by Python client software for analysis. All the sensors and transmission units are connected to one Arduino Uno board for data collection, signal processing and data streaming, Figure3.7.1 shows the sensor circuit diagram.

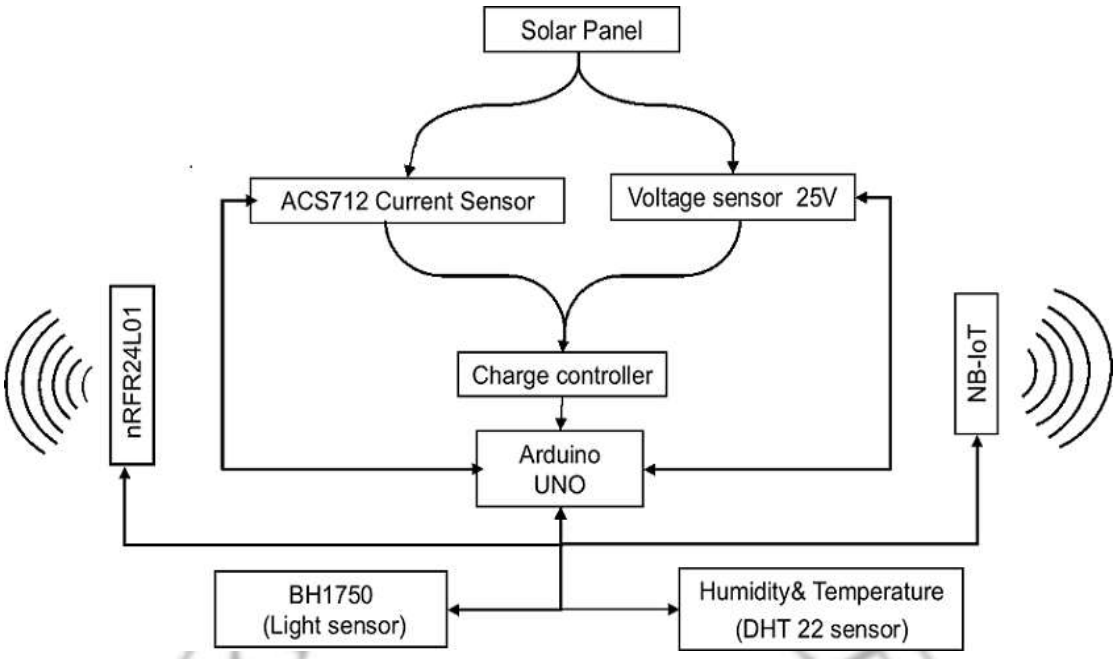

Figure 3.7-1: Sensor circuit diagram

3.8 The system energy consumption

Finally, it needs to be observed that the system consumes energy during running and sleeping modes. A sleeping mode is the state where the motors are not running to rotate the panel. The consumed energy in 24 hours can be estimated by calculating the consumed energy in each operation cycle (motor moving + sleeping), E_{cons} and is defined as:

$$E_{cons} = V_R \times I_R \times T_R + V_S \times I_S \times T_S \qquad 3.5$$

where *V*, *I* and *T* denote voltage drops, electrical currents and mode times The suffixes *R* and *S* symbolize running and sleeping modes, respectively. In the system developed, the running time, T_R is set to 1 second while the sleeping time T_S is set to 14 minutes. Subsequently the total consumed energy in one day, then can be estimated as:

$$E_{system/day} = E\,E_{cons} \times \left[24hours / (T_S + T_R) \right], 120 \times E_{cons} \qquad 3.6$$

E_{cons}×(24 hours/(T_S+T_R)) or 120×P_{cons} for the proposed system. The net stored energy in one day is the one calculated from PV-syst software subtracting the consumed energy

3.9 The tools specification

In this section, the study explains the equipment and their specifications, which are used in this experiment. All equipment were purchased from the local market.

3.9.1 Monocrystalline solar cell

Monocrystalline solar cell is a P-N junction of single crystalline silicon, using photoelectric effect of semiconductors that is able to collect solar radiation and convert it into electricity (Gray, 2011). As the n region is heavily doped and thin that light can penetrate easily, and the p region is lightly doped so that most of the depletion region lies in the p side (Kayes, 2009). The electricity that is generated from solar energy is DC current form of electricity, and solar energy can be use directly, or can be use by battery storage. Table 3.9.1-1 illustrate monocrystalline solar cell specifications.

Table 3.9.1-1: Monocrystalline solar panel specification

Specification	Value	Specification	Value
Solar panel length	70 cm	Solar panel maximum power	50 Watt
Solar panel width	51 cm	Operating voltage (Vpm)	17.4 V
Solar panel area	3570cm^2	Operating current (Ipm)	2.85 A
Solar glasses area	-	Open circuit voltage (Voc)	22 .4V
Solar glasses thickness	-	Short circuit current (Isc)	3.04A

3.9.2 nRF24L01 antenna

The nRF24l01 antenna is a short range 2.4-2.5 GHz ISM band and chip ratio transceiver (Nordir semiconductor, 2008). It consists of integrated frequency synthesize, a power amplifier, crystal oscillator, a demodulator modulator and enhanced shock burst protocol engine. The output power, frequency channel and protocol setup are easily programmable towards ISP interface. That makes it a low current consuming equipment. Table 3.9.2-1 illustrates the nRF24L01 antenna specifications. The nRF24l01 antenna schematic is added in appendix A2.

Table 3.9.2-1: Specification of nRF24L01 antenna

Parameter	Value	Unit
Minimum supply voltage	1.9	V
Maximum output power	0	dBm
Maximum data rate	2000	kbps
Supply current in TX mode @ 0dBm output power	11.3	Ma
Supply current in RX mode @ 2000kbps	12.3	Ma
Temperature range	-40 to +85	°C
Sensitivity @ 1000kbps	-85	dBm
Supply current in power Down mode	900	nA

3.9.3 Solar charge controller

Solar energy battery charging is a unique and difficult challenge. That is as continually connecting to the charging current might cause overheating and possible explosion risk (Phocos, 2015). Therefore, the flow of electricity from PV-panel to battery and loads requires a solar charge controller (SCC). In solar power plant; the

SCC is an alternative solution that necessity to be used. The SCC is a device that controls amount of electric current, which drawn from or added to the battery. The SCC charge controller prevents from overcharging and deep discharging of the battery. It stops charging when the battery voltage is high and restarts charging when the battery voltage falls below a certain threshold. There are two common solar charge controllers: pulse width modulation (PWM), and maximum power point trackers (MPPT). PWM charge controller allows the current that the PV-panel generates to charge the battery up to the target voltage. When the battery reaches this target voltage, the charge controller quickly switches to disconnect between batteries to the PV- panel array to keep constant battery voltage. This charge switching prevents the battery from over charging. MPPT charge controller is an indirect connection between the PV panel and the battery that the connection includes DC/DC voltage converter. The MPPT charge controller can take over extra produced PV- panel voltage and converts it into extra current at a lower voltage without losing power. This is done through an adaptive algorithm. The adaptive algorithm follows the maximum energy of solar panel and then adjust the incoming voltage to hold the efficient amount of energy. Table 3.9.3-1 shows advantage and disadvantage of both PWM and MPPT solar charge controller.

Table 3.9.3-1: Beneficial and drawback of both PWM and TPPM solar charger controller

PWM	TPPM
33-50% cheaper than a MPPT charge controller	Highest charging efficiency (especially in coo climates)
Longer hold lifespan due to lower electronic component and less thermal stress.	Can be used largely up to 60-cell panel.
Small size	Possible to oversize panel to ensure enough charging in cold seasons.
Required more experience must size the PV panel and battery bank carefully	2-3 time more expensive than PWM controller
Does not efficient to use up to 60-cell panel	Sued with more electronic component in the greater thermal stress that caused shorter lifespan

3.9.4 Arduino microcontroller

Arduino microcontroller is an open source and logical programmable hardware devices, which is widely used in different applications to control electrical hardware devices. That includes internet of things, wireless sensor network, and robotics controlling (Kamel & Anissa, 2016). This study uses Arduino UNO, which is one of the latest microcontroller in a series of USB Arduino boards. Arduino UNO board is based on ATmega328. It combines many features that are needed for microcontroller hardware interaction. It can simply be connected to the computer with USB cable. It can work standalone while powered by an AC to DC adapter, or battery. Arduino UNO has 14 digital input and output pins. In the board design six pins are used as PWM output, six Analog input, 16 MHz Crystal vibrator, a USB connection, power jack, an ICSP header, and a reset bottom. The specification of the board is shown in table, 3.9.4-1

Table 3.9.4-1: Arduino UNO technical specification

Parameter	Value	Parameter	Value
Microcontroller	ATmega328	DC current for 3.3V pin	50Ma
Operating Voltage	5V	SRAM	2KB
Input voltage Recommended	7-12V	EEPROM	1KB
Input Voltage (limits)	6-20V	EEPROM	1KB
DC current per I/O pin	40mA	Clock speed	16MHz
Analog input pins	6		
Digital I/O pins	14(which 6 provide PWM output		
Flash memory	32kb of which 0.5 kb used by boot loader		

3.9.5 BH-1750 light sensor

BH-1750 light intensity sensor is commonly used to determine the solar tracker accuracy by considering maximum sun radiation that is fall onto solar cell (M. electronics, 2019). BH-1750 sensor measuring range's is (0-65535) lx, which lx is the lux symbol in IS system. As it drives the unit of illuminance and luminance emitted measuring luminous flux per unit area. However, in our system it was used mainly to monitor the environment condition. During practical measuring, the high brightness of the day sunlight in Bangkok causes a sensor to saturated (giving maximum output of 54612.5 lx). Therefore, it was covered by a polarizer glass to decrease the light intensity reaching the sensor. Table, 3.9.5-1 determines the maximum specification of BH-1750, and Table 3.9.5-2 shows the recommended operating conditions for BH1750.

Table 3.9.5-1: BH1750 sensor maximum ratting specification

Parameter	Value	Unit
Supply voltage	4.5	V
INT, SDA, DVI, SCL, Terminal voltage	-0.3 to +7	V
Operating temperature	-40 to +85	°C
Storage Temperature	-40 to +100	°C
SDA,INT, Sink current	7	µA
Power dissipation	0.25(Note 1)	W

Table 3.9.5-2: Recommended operating Condition for BH1750 sensor

Parameter	Min	Type	Max	Unit
Temperature	-40	-	+85	°C
Supply voltage	2.4	3.0	3.6	V
I^2CI/O voltage	1.65	-	-	V

3.9.6 Temperature and Humidity sensor type (DHT22)

This study added DHT22 sensor to measure the environment weather condition. The sensor can measure both temperature and humidity (Robotics, 2010). DHT22 sensor is able to read the temperature from -40ºC to +80ºC, and from (0- 100) % of humidity. Its reading error is 0.5º C in temperature and 2% in humidity.

3.9.7 Current sensor type (ACS712, 30A)

Acs712 sensor is an economical and precise solution for AC and DC current, this module has three ranges for different sensor chips (5A, 20A, and 30A) (R- Semiconductor, 2010). This study uses module 30A, to measure solar panel output current, and the current electricity from battery to consumer's devices. The

ACS-712 current sensor measurement range is (-30 to +30) Amps corresponding to the analog output, the supply voltage is 5Volt, and the scale factor is 66Mv per Amps.

3.9.8 Stepper motor

Stepper motor is a discrete step motor that moves one specific step at a time. The stepper motor has different sizes with different voltage supply (Handson, 2010). This system uses 17HS4401S a 12volt bipolar stepper motor, which is able to rotate 10kg weight. Table 3.9.8-1 illustrates the stepper motor characteristics.

Table 3.9.8-1: Stepper motor specification

Parameter	Value	Unit
Motor type	Bipolar	Stepper
Step angle	1.8	deg.
Holding torque	40N	Cm
Rated current /phase	1.7	Amps
Phase resistance	1.50	hmt +/- 10 %

3.9.9 DC-Motor

The DC-motor or direct current motor is commonly used actuator for producing continuous movement that rotation speed can be easily controlled (Irtawaty & Ulfa, 2018). DC-motor has different sizes, this research used a small size 12V DC-motor, it is able to hold and rotate 12kg weight, it a low power consumer.

3.9.10 L298N Motor driver

This motor driver is a dual H-Bridge bidirectional DC-motor driver that is based on a very popular L298 H-Bridge motor driver integrated circuit

(ST Microcontroller, 2000). The L298N motor driver has four logical input pins, two pair's output pins, 5V and 12V power pins, and two enable pins. The circuit allows to easily and independently control one stepper motor or two DC-motor in both two directions. This motor driver can be easily programmed with Arduino, and can supply 5V power. Table 3.9.10-1 illustrates L298N motor driver specification.

Table 3.9.10-1: L298 motor driver specification

Parameter	Value	Unit	Parameter	Value	Unit
Input voltage	3.2~40	$Volt_{dc}$	Maximum power consumption (in temperature 75 °c)	20	W
Power supply	5 - 35	volt	Storage temperature	-25 ~+130	°C
Peak current	2	Amp`	On- controller board Output supply	5	V
Operating current range	0~36	Amp	Size	3.4×4.3×2.7	Cm

CHAPTER 4

DATA COLLECTION

4.1 Result and analysis of implementation

The system is designed to operate fully on the stored energy in the battery in Figure 1e. That includes providing excess energy for basic electricity usage as well as environmental monitoring. Hence, minimizing the power consumption during the operation time is required particularly for motor rotation. One way to reduce motor power consumption is through rotation in discrete steps rather than following the continuous movement of the sun. For instance, figure 4.1.1 illustrates the relationship between 30 and 60 minutes stepwise tracking system and misfit angle. In position 4.1- 1a the solar panel is normal towards the sun. In position 4.1-1b the angle between the solar radiation and the panel surface is 75°. In position 4.1-1c it is 60°. Therefore, the misfit angle is the angle the sunrays makes on the solar panel that rotates by the motor on a stepwise running. At the first time of the period the PV-panel is normal to the sun surface and there is no misfit angle. At the end of rotating time the sun radiation makes a finite angle on solar panel. Thus, the misfit angel effect on the output energy in a stepwise tracking system, can be determine by following equation.

$$E_{efficiency} = \cos\alpha \times 100\% \qquad 4.1$$

Where; $E_{efficiency}$ is amount of solar radiation that falls on solar panel at the end of stopping time of tracker, and $\propto$ is the misfit angle of the stepwise tracking system.

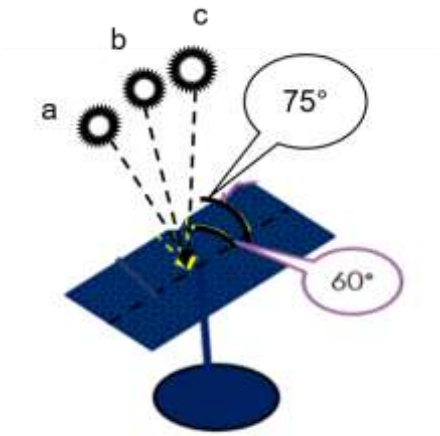

Figure 4.1-1: Misfit angle affect's on solar panel output efficiency

The step time though needs to be selected such that the system sustains output similar to continuous tracking movement. To determine the needed step time delay, the solar panel ratio and the misfit angles, which are explained below, when the motors run stepwise in both elevation and azimuth angles with delay periods varying from 0 to 60 minutes as depicted in Figure 4.1-2. The misfit angle α, is the angle the sun rays make from the normal to the surface of the solar panel. The solar panel ratio is the cosine of the misfit angle. It determines the ratio between the solar coverage area when the panel is tilted and the normal to the sun. As earth rotates once every 24 hours, every hour corresponds to 15^{o} of rotation or 0.25^{o} per minute. The calculations in Figure 5 show that a step time of up to 15 minutes sustains a solar panel value that is at least 99 % of the maximum amount of captured sun rays, which corresponds to a maximum misfit angle of 3°. Hence, in the experiment, a step delay of 15 minutes is implemented.

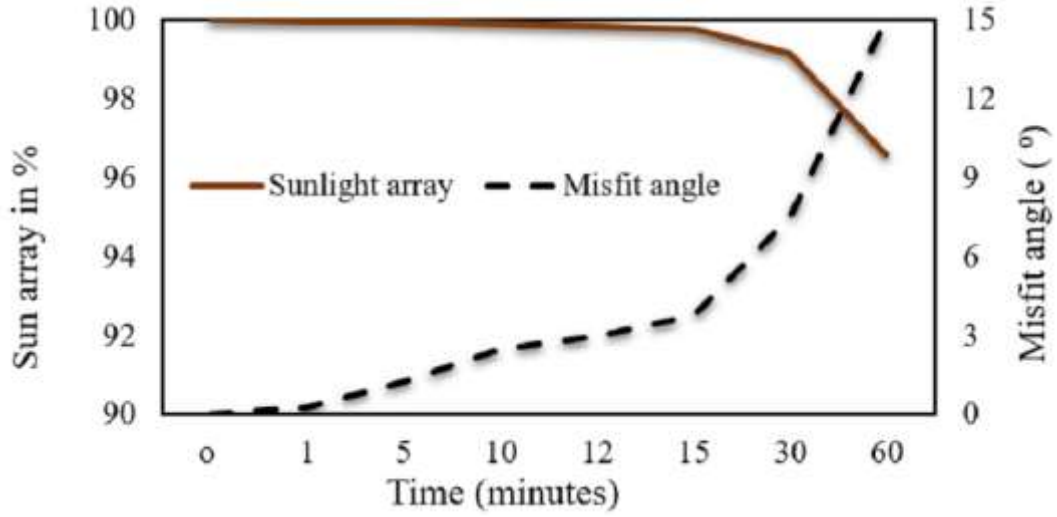

Figure 4.1-2: Motor step delay running and uneven angle

In the presented experiment, the panel is installed at location 13.986º latitude and 100.525028º longitude, which is near to the equator. The data for both the static panel and a panel with two axis solar tracking were collected over a period of nine months. Figure 4.1-3a depicts the measured output power for both static and tracking system over seven hours a day. This study used the same solar panel for both tracker and static system, and the measurements were done on two alternating days, one day for the static case and the other day for the tracking system. The measurements were done on two alternating days, one day for the static case and the other day for the tracking system. The days have similar weather conditions as illustrated in Figures 4.1-3b and 4.1-3c for humidity and temperature, respectively. The results indicate that the average PV-panel's output power is 45 Wh for the tracking system and 38Wh for the static panel. This corresponds to a total energy generated in 7 hours within one day of 315 Wh/day and 278 Wh/day, respectively. The data was measured on 17-18 of September where the sun radiation is received at an angle of 83° in the static panel

from the south. With a small misfit angle during this period, the amount of generated energy is almost the same amount of energy in both static panel and tracking system. Hence, the generated energy by the tracking system is 13% more than that of the statics panel.

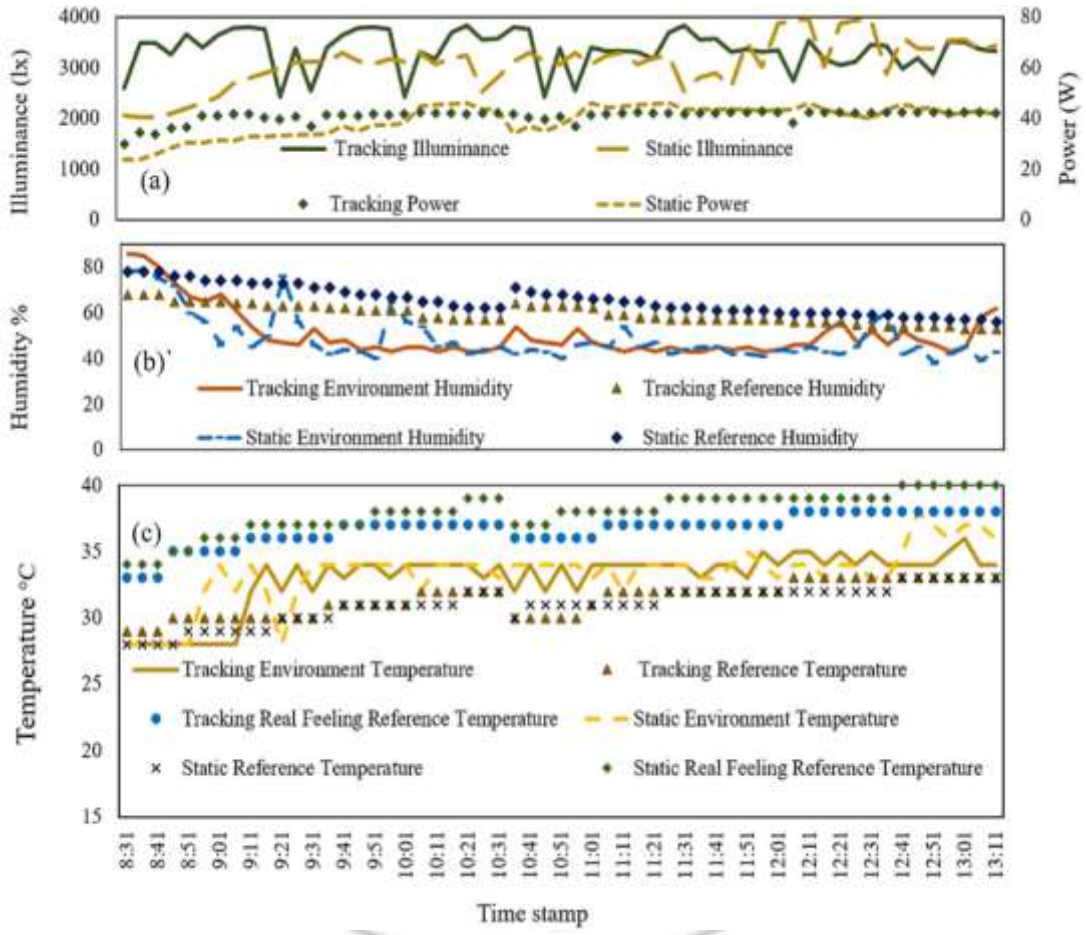

Figure 4.1-3: Comparison of solar panel output energy in both solar tracking system and static panel.

It is worth noting that, in the tracking system, each motor runs for one second and sleeps for 15 minutes. Using this model of operation and Equation 5, the power consumed by the motors and the circuits is calculated from the values measured by the current and voltage sensors. In each operation cycle the current raises to I_R = 560 mA during running time and decreases to I_S = 30 mA during sleeping time. During

running and sleeping, voltages are set to be equal, i.e. V_R = V_S = 12 V. The total consumed power in one day can be calculated from Equation 5 by setting T_R and T_S to 0.03 hours and 23.97 hours, respectively, which corresponds to 1 second operation time followed by 15 minutes sleeping time

$$E_{cons} = (0.56\text{A}\times0.03\text{h}+0.03\text{A}\times23.97\text{h})12\text{V}=8.76\text{Wh}$$

To include the weather effect, several conditions can be considered: sunny, cloudy, partially cloudy and rainy. However, this study focuses on comparing the performance between sunny and rainy days. As shown in Figure 4.1-4a, the generated power was measured over 7 hours on both sunny and rainy days. The environment's humidity and temperature were measured and compared to the online provided weather information in Figures 4.1-4b and 4.1-4c (labelled reference). Using monocrystalline solar cells, a total energy of 293 Wh and 47 Wh were generated on sunny and rainy days, respectively while using the tracking system. Although the light intensity on rainy days is, on average, 25% of that on sunny days, the monocrystalline solar cell panel was able to generate energy that is at least five times higher than that consumed by the motors and the electrical circuitry. This result supports the original choice of a monocrystalline solar panel over polycrystalline panels. As the open-loop solar tracking system is the best option to output a maximum amount of solar power in different weather conditions.

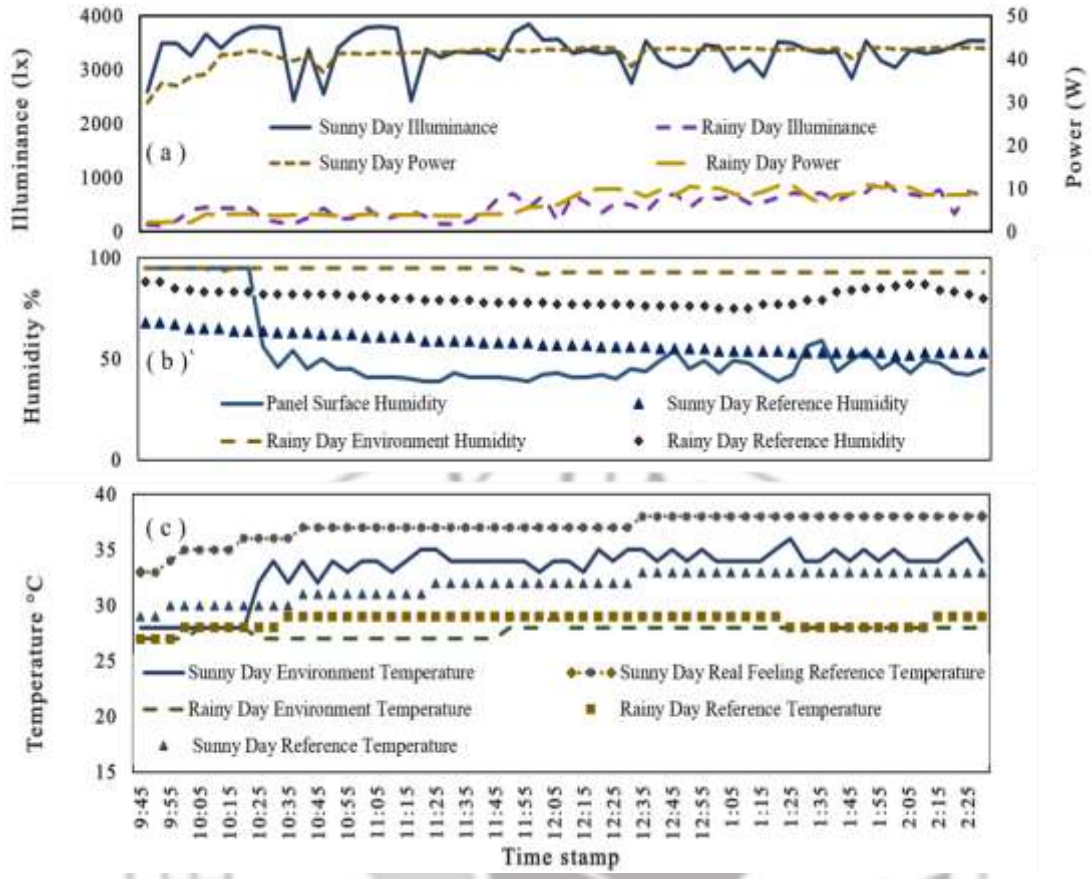

Figure 4.1-4: Comparison of solar panel output energy on sunny and rainy day

One practical factor that can affect the system efficiency is the solar panel's surface temperature. The measured output voltage decreases significantly with increasing temperature (Fesharaki & Dehghani, 2011). To monitor this effect, two temperature sensors were used, namely one for environment and one for the solar panel itself. Figure 4.1-5 shows a noticeable difference in temperature between the environment and the PV-panel area that was measured over a period of 4 hours around noon on a sunny day. The plots show that the panel temperature can reach 17^{o} C higher than the environment.

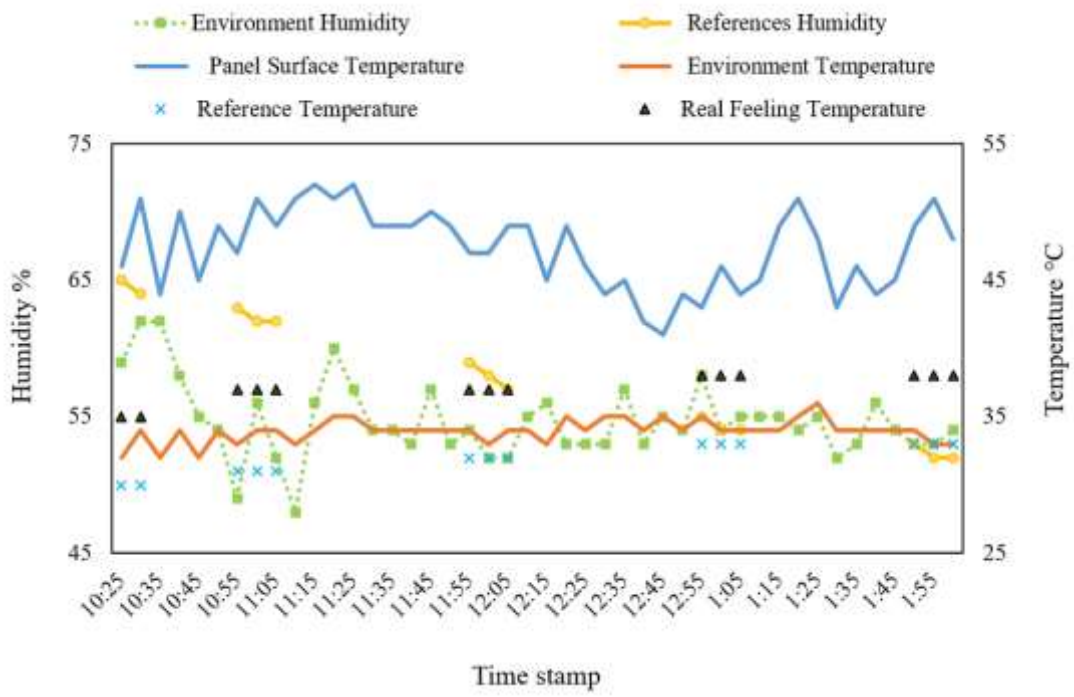

Figure 4.1-5: Difference temperature between solar panel and environment

Figure 4.1-6a denote that raising temperature causes the solar panel output voltage to drop significantly, but Figure 4.1-6b shows the PV-panel output current does not affected in temperature rising as well as output voltage is. In addition, long lasting temperature without controlling is caused to decrease the solar panel life.

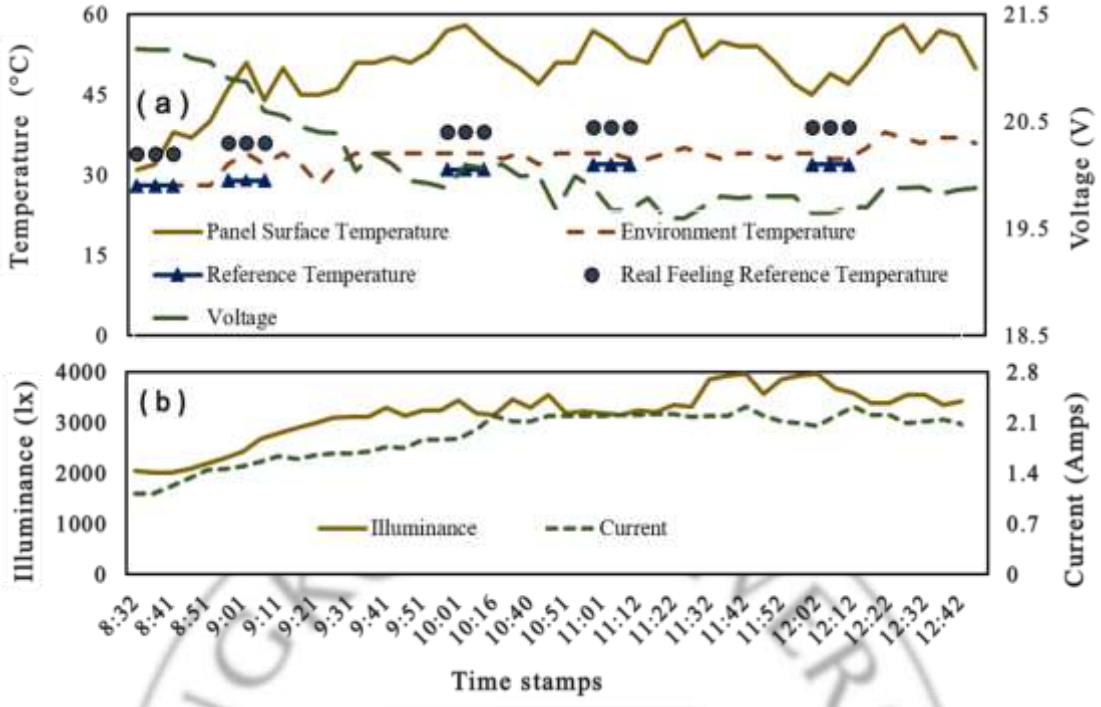

Figure 4.1-6: Comparison effect on solar panel output voltage

In order to test the system over long varying weather conditions, data were stored over nine months during April 2019 to January 2020. The generated energy is calculated per month and plotted in Figure 4.1-7 in comparison to calculations. Here obtained with PV-syst software. To acquire the needed calculations, the software requires defining the solar panel location by considering longitude, latitude, albedo, tilt, and zone time. It also requires setting the amount of demanded solar power in Watt, as well as the number and type of the solar cell with defining dual-axis tracking system. The software output includes produced useful energy, PV-panel loss, and the output power every month of the year as shown in Figure 4.1-7. It is worth mentioning that, for the experimental graphs in Figure 4.1-7, the output energy was measured over 7 hours daily for nine months due to the presence of obstacles in the areas. However, Bangkok has at least 11 hours of daily sun during all seasons. The

monthly calculated sunny hours are different from the software and the practical. For example, the sunny hours in Bangkok are 255 to 210 hours in April. This difference in calculation for the operating times caused the difference in the trends as shown in Figure 4.1-7. To take this into account, the data was interpolated every day to fit the remaining afternoon time. Additionally, the experiment was not performed continuously every day due to weekends and holidays. To estimate the output energy in one month, the average daily energy was calculated as.

$$\mathrm{E_{Month}} = \frac{\sum_{1}^{n} \mathrm{E_N}}{\mathrm{N}} \times \mathrm{month_{days}} \qquad 4.2$$

where E_{Month} is the total obtain energy per month, and N is the number of the days that the solar energy was collected during one month. $\sum_{1}^{n} E_N$ is the total measured energy during the nth day out of the N days over which the experiment was conducted during a particular month. For instance, consider equation 7, the total generated energy in September 2019, which was measured on 11 different days of September using the solar tracking system, the following calculation was made.

$$E_{Month} = \frac{2354.624}{11} \times 30 = 6.422 \frac{kWh}{Month}$$

This approximation could be the main reason of the obvious difference between the measurement in practical and simulation in Figure 4.1-7.

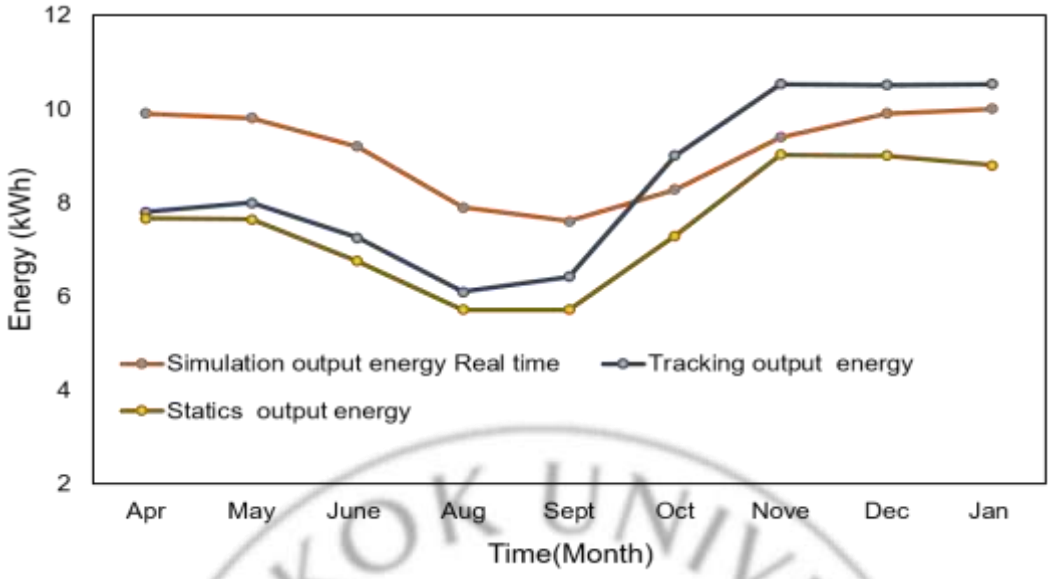

Figure 4.1-7: Comparison of generated energy per month over a period of 9 months

Finally, Figure 4.1-8 depicts the produced energy by the tracking system and the static panel, and this in different weather conditions and different seasons of the year. The figure clearly indicates that the obtained energy using a tracking system is higher than that of a static panel on sunny days. On rainy days, however, the outcome is comparable. On cloudy days, the condition changes along the day from sunny to cloudy and vice versa in case, especially in the case of partly cloudy conditions. Also, light scattering by the clouds sustains some sort of directionality. Hence the tracker increases the solar panel efficiency.

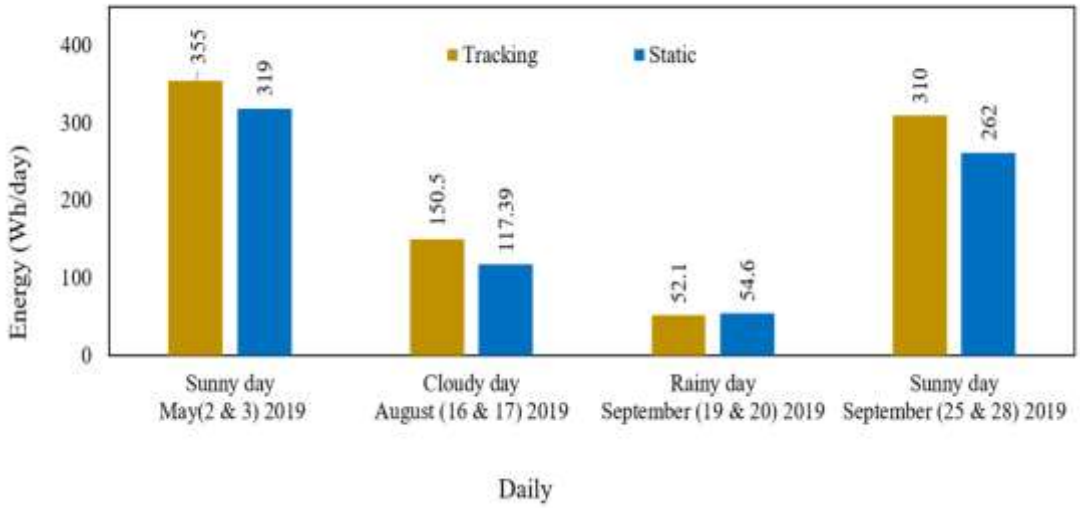

Figure 4.1-8: Comparison output energy in both tracking system and static panel in different weather condition

4.2 Comparing present solar power plant with commercial

In order to evaluate the cost effectiveness of this system, a breakdown of the components cost is compared to one commercially available sun tracker vendor [24]. The results are scaled in order to consider the developed solar power plant size. In this calculation, minor extra tools are not taken in consideration as their cost is negligible. Table 4.2-1 shows the solar tracker tools cost in both the commercial vendor and presented system.

Table 3.9.10-1: Comparison of solar tracker tools in manufactories and this experience

Solar tracker cost for commercial vendor			Solar tracker cost for the developed system		
Item	Unit	Price per unit $	Item	Unit	Price per unit $
Linear actuator 12V	1	40	Stepper motor ,12V	1	
motor	1	100	IMS bearing	3	
Dual-Axis solar tracker	1	100	Screw and rod	1	
Dual-Axis slewing drive			DC motor, 12V	1	
bearing	1	40	PWM Charge controller	1	
RS232 Ethernet server			Solar panel	1	
converter	1	12	monocrystalline 50W		
DC motor azimuth tracker	1	45	Battery , 12V~24hMD	1	
Clamp assembly SM3	1	35	Arduino UNO	1	
Solar panel			L298 motor driver	2	
monocrystalline 50W	1	65	DS1307 Real Time Clock	1	
Battery , 12V~24hMD	1	11			
Charger controller PWM					
Total		$448			$193

4.3 The experiment Challenge

During process of sensor circuit data collecting there were many challenges. One of the main issues was ACS217 current sensor data reading. As mentioned in figure 3.7.1 of chapter, three current sensors were installed between solar panel and the charge controller to measure the output current. Similarly, a 12V Battery is directly connected to the charge controller too. The problem of the sensor was being short-circuited and many times burned resulting in errors in the recorded data. Replacing the current sensor replaced many times did not solve the problem permanently. Therefore, the current was measured using multi meter, which was not according to the data collection period manual.

4.4 Payback time of solar panel

The component that used in this study is may low quality than solar tracking system but the advantage of this system is that it sued simple components. For example, one Arduino is used to control all tracking system, which is easy to replace, and can work for all lifetime of solar panel. According to different research and factories standard, the solar panel average lifetime are 20-25 years. Thus, it is important to determine that solar panel production decrease during lifetime due to chemical reaction exposed to the sun light [25]. Many research result shows that 0.5% of output solar power each year. According to the effects and in consider to 50 Watt solar panel the payback time and output energy is calculated for 6 months of each year. Table 4.4-1 shows payback time and output power of each month separately.

Table 3.9.10-1: Payback time of 50 Watt solar panel

Month	First Year	Second Year		24^{th} year	25^{th} year
Apr	7.801	7.76	…	6.86	6.82
May	7.995	7.95	…	7.03	6.99
June	7.25	7.21	…	6.38	6.34
Aug	6.093	6.06	…	5.36	5.33
Sept	6.422	6.38	…	5.65	5.62
Oct	9.003	8.95	…	7.92	7.877

Total amount of generated energy trend in 6 months of each year for 25 years which determine payback time solar panel is shown in Figure 1.

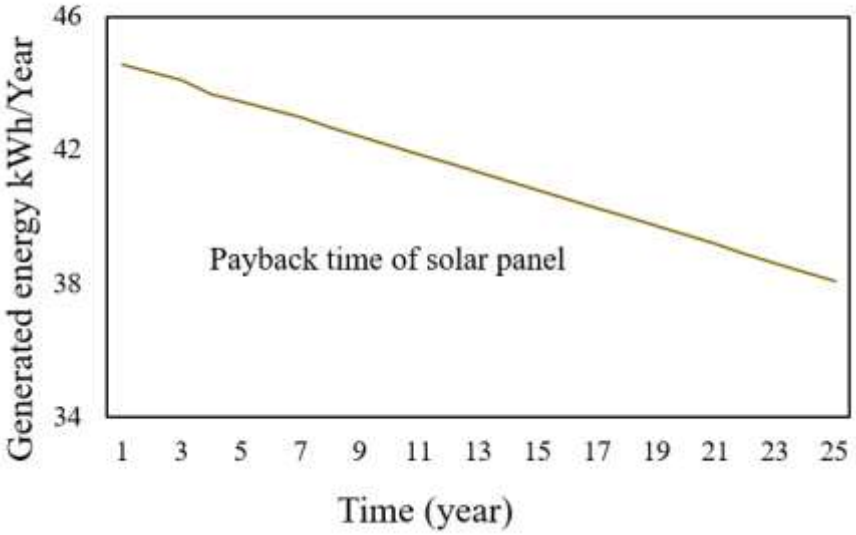

Figure 4.4-1: Payback of solar panel

CHAPTER 5

CONCLUSIONS

This thesis presented a dual axis, open-loop tracking solar system using a 50 Watt monocrystalline solar panel and two motors, namely DC and stepper motor. The motors are controlled by a single Arduino board programmed for the real time tracking of the sun's position. A 12V battery is mounted to store solar energy by using a PWM solar charge controller that prevents the battery from overcharging. Multiple sensors were used to collect environment data, which were transmitted using nRF24L01 antenna and narrow band wireless communication link in order to monitor the system's performance as well as the environment. Misfit angle of stepwise tracking system was estimated that in the system the operating time of every step was 14 minutes. On average, the solar tracker consumed 8.7 Whr/day energy. The different between PV-panel surface and environment temperature were (53°C, 36°C) which it is 17°C higher at average. Thus, it caused the output voltage decrease. Experimental data were collected in both a solar tracking system and a static PV- panel, and this in different weather conditions. The results over a nine months experiment period showed that the panel with the open-loop tracking system produced 18% more energy than the statistic panel (i.e on average 6.422.kWh/month, compared to 4.89 kWh/month). In rainy weather the PV-panel generated 47Wh/day which is 25 % of sunny days output energy. The results seem to follow the calculated power based on PV-Syst software with the difference attributed to the interpolation of the data during the non-operation period.

BIBLIOGRAPHY

Arunpold, S., Tripathi, N.K., Rajesh, Chowdhary, V., and Raju, D.K. (2014). Comparison of GPS-TEC Measurements with IRI-2007 and IRI-2012 Modeled TEC at an Equatorial Latitude Station in Bangkok, Thailand. *Journal of Atmospheric and Solar Terrestrial Physics, 117,* 88-94.

Aigboviosa, A.P., Anthony, A., Claudius, A., Uzairue,S., Timilehin, S., & Imafidon, V.(2018). *Arduino based solar tracking system for energy implement of PV-solar panel*. Department of electrical and information engineering covenant university, Nigeria. International conference on industrial engineering ond operation management Washington DC, USA.

Allegro Microsystem. (2019). *Fully Integrated, Hall Effect-Based Linear Current Sensor with 2.1 Kvrms Voltage Isolation and a Low-Resistance Current conductor*. *ACS712-DS, Rev.6.* Retrieved from www.allgeromicro.com.

Bhuvaneswari, P.T.Y., Balakumar, R., V., & Balamuralidhar, P. (2009). Solar Fenergy harvesting for wireless sensor networka. International conference on computational intelligence communication systems and networks.

Carballo, A.J., Bonilla, J., Roca, L., & Beranguel, M. (2018). New low-cost solar tracking system open source hardware for based on educational purposes, solar energy, 174, 826-836.

Chin, C.S., Babu,A., & McBride, W. (2011). Design, modeling and testing of a standalone single axis active soar tracking using MATLAB Simulation, *Renewable energy. 36(11),* 3075-3090.

Chong, K.K., & Wong, C.W.(2011). Application on-axis general sun tracking formula in open loop sun tracking syste for achieving tracking accuracy of below1 mrad. *International journal of engineering. 1(1), 25-32.*

Christopher K., Thomas, S., & Nikolaos, M. Exergy analysis of renewable energy sources. *Fuel and energy. Abstracts.44(3)*, 295-310

Director General Department of Agricultural West Australia. (2004). Methods of calculating solar position and length including computer programs and subroutines. Resource management technical report, No, 137.

Dahiya,M., 2017. A short range wireless network: Bluetooth. *International journal of advanced research in computer science. Maharja surajmal institute. India, 8 (3),* 37-40.

D-Robotics semiconductor. (2010). *Humidity and Temperature Sensor, [Online], available www.droboticsonline.com*

Ershad, A.M. (2017). Institutional and policy assessment of renewable energy sector in Afghanistan. *Journal of renewable energy*.

Ferdaus, R. A., Mohammed, M, A., Rahaman, S., & Salehin, S. (2014). Energy efficient hybrid dual axis solar tracking system. *Journal of renewable energy, 1-12.*

Fesharaki, V. J., Dehghani, M., Fesharaki, J. J., & Tavakoli, H. (2011). The effect of temperature on photovoltaic cell efficiency. *Proceedings of the 1st international conference on emerging trends in energy conservation - ETEC Tehran, Tehran, Iran, 1-6.*

Garcia, L.R., Barreiro, P., & Robla, J.I. (2008). Performance of ZigBee-based wireless sensor node for real time monitoring of fruit logistics. *Journal of food engineering, 87,* 405-415.

Gerro, P., & Robert, D. (2015). Solar tracking high precision solar position algorithm, programs, software and sources-code for computing the solar vector, solar coordinates and sun angles in microprocessor, plt, arduino, pic and pc-based sun tracking devices or dynamic sun following hardware. Solar Books, 66-70.

Gray, J, L. (2011). The Physic of solar cell. Purdue University, West Lafayette, Indiana, USA. Photovoltaic Science and Engineering. V(2), 83-127.

Guala, F., Mansourian , A., & Groth, R. (2015). Sun position and PV panels: a model to determine the best orientation. Student's thesis series. nr: 360. Department of Physical Geography and ecosystem Science. Lund University. Sweden.

Handson.T. (2010). *17HS4401S Stepper Motor. [Available]* *www.handsontec.com*.

Hou, H., Wang, M., Yang, Y., Chen, S., & Hu, E. (2010). Performance analysis of a solar–aided power generation (sapg) plant using specific consumption theory. *Science china technology sciences, 59(2),* 322-329.

Huynh, D, C., Nguyen, T, M., Dunnigan, M, W., & Mueller, M, A. (2013). *Comparison between open - and close- loop trackers of a solar photovoltaic system.ieee confernccе on clean energy and technology(ceat), 128-133.*

Irtawaty,S,A.,.& Ulfa,M. (2018). Rancang bangun sistem daur ulang minyak goreng bekas berbasis algoritma fuzzy logic. *Jurnal simetris, V (9),* 2252-4983.

John , A.D., & Beckman, W.A. (2013). Solar engineering of thermal. *Solar energy laboratory university of wisconsin-madison, vol.4, 1-6.*

John, A.D., & William, A.B. (2013). Solar Engineering Thermal Processes. *Fourth Edition. Solar Energy Laboratory University of Wisconsin-Madison.*

Joshua, F.E, & Matthew, S.R. (2015). Every smart phone is a backscatter reader: modulated backscatter compatibility with Bluetooth 4.0 low energy devices. IEEE intenational confrance on RFID.Department of electrical engineering, University Washington, 78-85.

Jurdak, R., Antonio, G.R., & Gregory, M.P. (2010). Radio sleep mode optimization in wireless senor network. IEEE transactions on mobile computing, 9(7), 955-068.

Jumaat, S.A., Azlan Tan, A.A., & Abdullah, M.N. (2018). Horizontal Single Tracker using Arduino Approach. *Indonesian Journal of Electrical Engineering and Computer Science, 12(2)*, 489-496.

Kabalci Y., & Ali, M. (2019). *Emerging LPWAN Technology for smart environment. An outlook. 2019.1st global power*. Energy and communication conference (GPECOM).

Karmaker, A, K., Rahman, M., Hossain, A., and Ahamed, R., 2019. Exploration and corrective measures of greenhouse gas emission from fossil fuel power stations for Bangladesh. *Journal of cleaner production, Vol. 244*, No.11865

Kandasamy, C, P., Prabu, P., and Niruba, K. (2013). *Solar Position Assessment using PYSYST Software*. International Conference on Green Computing Communication and Conservation of Energy (ICGCE), 667-672.

Kayes.B.M., 2009. Radial pn junction, Wire Array Solar Cell. In Partial Fulfillment of the Requirement for the Degree of Doctor of Philosophy. California Institute of Technology Pasadena, United State of America.

Kamel. K. &Anissa. K. (2016). Design and Implementation of Microcontroller Based Controller for direction and Speed of a Robot using Arduino. Master Thesis. Faculty of Technology the University of Echahid Hamma Lakhdar El Oued. Algeria, 29- 40.

Key world energy statistics. (2017). International *energy agency (IEA).*

Kevrak, S., & Gunduzal, M. (2010). Theoretical and experimental performance investigation of a two-axis soar tracker under the climatic condition of Denizli, Turkey, 332-336.

Lee, C.D., Huang, H.C., & Yeh, H.Y. (2013). The Development of Sun- tracking system using image processing. *Journal of sensors. 13(5),* 5446-5459.

Lee, C.-Y., Chou, P.-C., Chiang, C.-M., & Lin, C.-F. (2009). Sun Tracking Systems: A Review. *Journal of sensors, 9(5), 3875–3890.*

Melo, A.G., Filho, D.O., Junior, M.M.O., Zolnier, S., & Ribeiro, A. (2017). Development of a closed and open loop solar tracker technology. Acta Scientiaru, 39(2), 177-183.

Mohammad, E.H.G,. Amith, K., Belayat, H., & Rayaan, A. (2019). A low- cost closed-loop solar tracking system based on the sun position algu rithm. *Journal of sensors, 11.*

Nikoukar, A., Raza, S., Poole, A., Gunesh, M., & Dezfouli, B. (2018). Low-Power Wireless for the internet of things. *Journal of Standard and Application*, 67893- 67924.

Nordir semiconductor. (2008). *Nrf24l01 Antenna production specification. Norway, 8- 36,* www.nordicsemi.com.

ÖZturk ,A. Alkan ,S. Hasirci, U. & Tosun, S. (2016). Experimental performance comparison ot a 2-axis sun tracking system with fixed system under the climate conditions of Duzce Turkey. *Turkish Journal of Electrical Engineering and computer science, 24,* 4383-4390.

Phocos. (2015). Comparing PWM & MPPT Charge Controllers. North America. www. Phocos.com.

Prajapati, V., & Patel.R. (2015). Development of dual Axis solar tracking system. *International journal for scientific Research and Development. 3(08),* 702- 705.

Raheleh,R., Meysam, S, K., Hasanuddin, L. & Dalia, S. (2017) An overview of Afghanistan's Trends Toward Renewable and Sustainable Energies Renewable and Sustainable Energy Review,76, 1440-1464.

Ralph E.H., Hans, H.R. & Ken, G. (2003). Carbon Emission and Mitig.tion Cost Comparisons between Fossil Fuel, Nuclear and Renewable Energy Resources for Electricity Generation, *Energy Policy, 31*, 1315-1326.

Rubio, A.J., Cerdan, C.F. & Suardiaz, M.J. (2019). Design and implementation of a mixed IoT LPWAN network architecture. *Journal of sensors, 19(3),* 675.

R-Semiconductor, 2010, *BH1750 Digital 16bit Serial Output Type Ambient Light Sensor [Online]* *WWW.rohm.com*.

Same, S., Srpcic, G., Kavsek, D., Bozicnik, S., & Letnik, T. (2017). Dual –axis Photovoltaic Tracking System Design and Experimental Investigation, *Energy, 139,* 1267-1274.

Sadeq,F. (2017). Design and Implementation of Automated Solar Tracking system, unpublished Master.D, dissertation..BellVille: Bangladesh University of engineering and technology Dhaka, Bangladesh.

SAT-CONTROL, (2016). Solar tracker [Online] www.solar-motors.com

Selvakumar, R. (2016). Energy efficiency shift based sleep scheduling mechanism for wireless sensor network deployment in rescuebots. *International Journal of applied engineering research ISSN 11(9). 6489-6496.*

Singh, R., Kumar, S., Gehlot, A., & Pachauri, R. (2018). An Imperative Role of Sun Tracking in Photovoltic Technology. *Renewable and Rustaiable Energy Reviews. 82*, 3263-3287.

Sirigauri, N., Raghav, S., Nikhil, R., & Mounik, D.R. (2015). Design and implementation of Dual Axis Solar tracking system. *Journal of Engineering and Applications*. Department of Electrical and Electronics Engineering, BMS Collage of Engineering, Bangalore-560019, India. *5(5)*, 48-51.

Singh, R., Kumar, S., Gehlot, A., and Pachauri, R. (2018). An Imperative Role of Sun Tracking in Photovoltic Technology. *Renewable and Rustaiable Energy Reviews, 82*, 3263-3287.

Sierke, J., Kusakana, K., & Numbi, B.P. (2017). A review of solar photovoltaic system cooling technology. *Renewable and sustainable energy review. Vol.79,* 192- 203

Solaun K., & Cerdá, E. (2019). Climate change impacts on renewable energy generation. A review of quantitative projections. *Renewable and sustainable energy Reviews, 116,* 109415.

ST Microcontroller, 2000, *L298 Dual H-Bridge motor driver. Dual H-Bridge Motor Driver.[online]* www.st.com.

Svensson, E., (2016) Evaluation of cost competitiveness and payback period of grid-connected photovoltaic systems in Sri Lanka, Bachelor of Science Thesis Product Realization Industrial Engineering and Management Royal Institute of Technology Stockholm, Sweden. PP 28-32.

Tarng, W., Ou, K.L., Lu,Y.C., Shih, Y.S., & Liuo, H.H. (2018). A sun path observation system based on augment reality and mobile learning. *Mobile Information Systems*. Pp (1- 10).

Tarujyoti, B. (2012). Impact of Solar Energy in Rural Development in India. International Journal of Environmental Science and Development, Vol. 3, No.4, 334-338.

Wazed, S.M., Hughes, B.R., O'Connor,D., & Calautit,J.K. (2017). Solar driven irrigation systems for remote rural farms. Energy procedia.124, 184-191.

Weller B., Hemmerle C., Jakubetz S., & Unnewehr S. (2012). Photovoltaics, technology architecture installation. Birkhaauser, Basel.

Zhou Q., Zheng K., Hou, L., Xing, J. & Xu,R. (2019). Design and implementation of open LoRa for IoT ieee Access. 1-1.

APPENDIX

ARDUINO CODING

6.1 Tracking code

6.1.1 Tracker controlling code

In this section, the electrical circuit controlling code is added. That includes the code of one DS1307 real time clock sensor and two L298N motor driver. Both motor drivers and DS1307 sensor are programmed by one Arduino UNO to control the tracker implementation. In the code, the operation time is one second every14 minutes.

```
/* ------------------------------------------------------- */
const int stepsPerRevolution = 200;
int dc_motor_count = 0;
int current_minutes = 0;
int last_minutes = 0;
/* ------------------------------------------------- */
#include <Stepper.h>
#include <Wire.h>
#include "DS1307.h"
#include <L298N.h>
#define DC_MOTOR_FORWARD  9
#define DC_MOTOR_BACKWARD  8
DS1307 clock;
int Hour = 0;
int Min = 0;
int Sec = 0;
/* ------------------------------------------------- */
// define L298N Sheild for stepper motor
Stepper myStepper(stepsPerRevolution, 3, 4, 5, 6);
/*-------------------------------------------------*/
int forward_count = 0;
int backward_count = 0;
String stepper_motor_direction = "forwards";
String dc_motor_direction = "forwards"
/* ------------------------------------------------- */
void setup (void)
{
setup_pins();
```

```
initial_motor_values();
setup_serial_port();
clock.begin();
read_time_date();
last_minutes=Min;
Serial.println(Min);
}
/* ------------------------------------------------- */
void loop( void )
{

read_time_date();
current_minutes=Min;
Serial.print(Hour);
Serial.print(":");
Serial.print(Min);
Serial.print(":");
Serial.println(Sec);
/* ------------------------------------------------------------ */
/* Check time morning or afternoon and set stepper motor direction */
if ( ( (Hour >= 8) ) && ( (Hour < 12) ) )
{
// Allow stepper motor to move forwards
stepper_motor_direction = "forwards";
} else if ( ( (Hour >= 12) ) && ( (Hour <= 16) )
{
// Allow stepper motor move backwards
stepper_motor_direction = "backwards";
} else
{
stepper_motor_direction = "none";
}
delay(60000);
if ( ( current minutes - last_minutes) >= 14)              // if 5 seconds have passed - need to take into
account that seconds go 0 to 59 and back    to 0
{
run_stepper_motor();
dc_motor_count = dc_motor_count + 1;
last_minutes= current_minutes;
}
 * ------------------------------------------------------------ */
  /*        DC-motor Run forward between 8:00 am and 3.59
   *        Run DC-motor once every 14 minute for 1000ms
   *        Run DC-motor for 8 hours
   *        Run backwards between 4:00 pm and 4:12:30 minute
   * ----------------------------------------------------*/
if ( ( (Hour >= 8) ) && ( (Hour < 16) ) )
{
// Allow dc motor to move forwards
dc_motor_direction = "forwards";
if ( dc_motor_count == 1)  // if 5 minutes (= 60 * 5 seconds) have passed
{
run_dc_motor();
dc_motor_count = 0;
}
} else if (((Hour >= 16)) && ((Hour <= 17)))
```

```
{
// Allow dc motor move backward
dc_motor_direction = "backwards";
if (dc_motor_count ==1/10 )           // if 5 minutes (= 60 * 5 seconds) have passed
{
run_dc_motor();
dc_motor_count = 0;
}
} else
{
dc_motor_direction = "none";
}
/* ----------------------------------------------------------*/
if (current_minutes ==59)
{
Serial.println("Current seconds = 60");
last_minutes =0;
}
}
/*-------------------------------------------------------------*/
void initial_motor_values( void )
{
Serial.println("Set initial motor values");
digitalWrite(2, HIGH);
digitalWrite(7, HIGH)
}
/*-------------------------------------------------------------*/
void run_stepper_motor( void )
{
Serial.print("Run stepper motor -> ");
Serial.print(stepper_motor_direction);
Serial.print(" : ");
Serial.print(forward_count);
Serial.print(" : ");
Serial.println(backward_count);
/*-------------------------------------------------------------*/
if (stepper_motor_direction == "forwards")
{
if(forward_count == 0);
{
myStepper.step(stepsPerRevolution);
delay(1000);
}
/*-------------------------------------------*/
} else
{
if (backward_count == 0)
{
myStepper.step(-stepsPerRevolution);
delay(1000);
}
}
}
/* ------------------------------------------------- */
void run_dc_motor( void )
{
```

```
Serial.print("Run dc motor -> ");
Serial.print(dc_motor_direction);
Serial.print(" : ");
Serial.print(forward_count);
Serial.print(" : ");
Serial.println(backward_count);
if (dc_motor_direction == "forwards")
{
if(forward_count==0)
{
digitalWrite(DC_MOTOR_FORWARD, HIGH);
digitalWrite(DC_MOTOR_BACKWARD, LOW);
delay(1000);
digitalWrite(DC_MOTOR_FORWARD, LOW );
digitalWrite(DC_MOTOR_BACKWARD, LOW );
}
} else
{
if(backward_count==0)
{
digitalWrite(DC_MOTOR_FORWARD , LOW);
digitalWrite(DC_MOTOR_BACKWARD, HIGH);
delay(1000);
digitalWrite(DC_MOTOR_FORWARD , LOW);
digitalWrite(DC_MOTOR_BACKWARD, LOW);
}
}
}
/* ---------------------------------------------- */
void setup_pins( void )
{
myStepper.setSpeed(60);
Serial.println("Set-up Arduino pins");
/* ---------------------------------------------- */
 // Stepper motor output
pinMode(2, OUTPUT);
pinMode(5, OUTPUT);
pinMode(DC_MOTOR_FORWARD, OUTPUT );
pinMode(DC_MOTOR_BACKWARD, OUTPUT );
}
/*-------------------------------------------------------------*/
void read_time_date( void )
{
//Serial.println("Read RTC time and date");
clock.getTime();
Hour = clock.hour;
Min = clock.minute;
Sec = clock.second;
}
/*-------------------------------------------------------------*/
void setup_serial_port( void )
{
Serial.begin(9600);
Serial.flush();
Serial.println("Set-up serial port");
}
```

```
// ------------------------------------------------------------------------------------------------------------------------------------------
------------------------------------------------------------------------------------------------------------------------------------------//
```

6.1.2 Sensors reading code

This appendix shows the code for the sensors circuit and the NB-IoT are programmed in one Arduino ONU to transmit environmental data to internet. The operation cycle is 5 minutes.

```
//    ------------------------------------------------------------------------------------------------------------------------------------------
------------------------------------------------------------------------------------------------------------------------------------------ //
#include "Magellan.h"
#include "DHT.h"
#define DHTTYPE1 DHT11
#define DHTTYPE2 DHT11
#define VIN1 A0
#define VIN2 A2
/*-----------------------------------------------------------------*/
#include <Wire.h>
#include <BH1750.h>
BH1750 lightMeter(0x23);
/*-----------------------------------------------------------------------------------------------*/
int offset1 =20;    //25 volat, voltage sensor to measure the laod consumming voltage
int offset2 =20;    //25 volat, voltage sensor to measure the laod consumming voltage
/*-----------------------------------------------------------------*/
const float VCC1   = 5.0;   // supply voltage is from 4.5 to 5.5V. Normally 5V.
const float QOV1 =   0.5 * VCC1;
const int model1 = 1;          // enter the model number (see below)
/*-----------------------------------------------------------------*/
const float VCC2   = 5.0;   // supply voltage is from 4.5 to 5.5V. Normally 5V.
const float QOV2 =   0.5 * VCC2;   // set quiescent Output voltage of 0.5V
const int model2 = 1;         // enter the model number (see below)
/*-----------------------------------------------------------------*/

float voltage1;      // internal variable for voltage
float cutOffLimit1 = 0.025;                    // set the current which below that value, doesn't matter.
Or set 0.5
float sensitivity1[] ={
        0.185,        // for ACS712ELCTR-05B-T
        0.100,        // for ACS712ELCTR-20A-T
        0.066,         // for ACS712ELCTR-30A-T
       };
/*-----------------------------------------------------------------*/
float voltage2;     // internal variable for voltage
float cutOffLimit2 = 0.025;             // set the current which below that value, doesn't matter. Or set 0.5
float sensitivity2[] ={
        0.185,        // for ACS712ELCTR-05B-T
        0.100,         // for ACS712ELCTR-20A-T
        0.066         // for ACS712ELCTR-30A-T
       }
```

```
/*-----------------------------------------------------------------*/
Magellan magel;
char auth[]="5ff181a0-892c-11e9-810a-f990cf998f9d";                    //key from Magellan
const int pin_dht1 = 2;
DHT dht1(pin_dht1, DHTTYPE1);
const int pin_dht2 = 3;
DHT dht2(pin_dht2, DHTTYPE2);
/*-----------------------------------------------------------------*/

String payload;
void setup()
{
Serial.begin(9600);
magel.begin(auth);                    //init Magellan LIB
lightMeter.begin();
//lightMeter.begin(BH1750_CONTINUOUS_HIGH_RES_MODE);
Serial.println(F("BH1750 Test"));
}
void loop()
{
int volt1 = analogRead(A1);
int volt2 = analogRead(A3);
/*-----------------------------------------------------------------*/
double voltage1 = map(volt1,0,1023, 0, 2500) + offset2;
voltage1/=100;
double voltage2 = map(volt2,0,1023, 0, 2500) + offset2;
voltage2/=100;
/*-----------------------------------------------------------------------------------------------------------*/
float voltage_raw1 =   (5.0 / 1024.0)* analogRead(VIN1);       // Read the voltage from sensor
voltage1 =  voltage_raw1 - QOV1 + 0.012 ;// 0.000 is a value to make voltage zero when there is no
current
float current1 = (voltage1 / sensitivity1[model1])/2;
float voltage_raw2 =   (5.0 / 1024.0)* analogRead(VIN2);       // Read the voltage from sensor
voltage2 =  voltage_raw2 - QOV2 + 0.012 ;  // 0.000 is a value to make voltage zero when there is no
current
float current2 = (voltage2 / sensitivity2[model2])/2;
/*-----------------------------------------------------------------*/
Float lux = lightMeter.readLightLevel();
//String rssi = magel.rssi();
float temperature1 = dht1.readTemperature();
float humidity1 = dht1.readHumidity();
/*-----------------------------------------------------------------*/
float temperature2 = dht2.readTemperature ();
float humidity2 = dht2.readHumidity();
/*-----------------------------------------------------------------*/
//payload in json format

payload = "{\"T1\":" + String(temperature1)  +",\"H1\":" + String(humidity1)+ ",\"L\":" + String(lux)
+",\"V1\":" + String(voltage1)+",\"C1\":" +
String(current1) + *",\"V2\":" + String(voltage2)+",\"C2\":" + String(current2) +",\"T2\":" +
String(temperature2) +",\"H2\":" +
String(humidity2) + "}";
magel.post(payload);          //post payload to Magellan
}
//-----------------------------------------------------------------------------------------------------------------
-----------------------------------------------------------------------------------------------------------------
-----//
```

6.2 Tracking data results for each month

This section provides tables of both solar simulation and experimental output. That includes the amount of monthly generated energy and average light intensity, temperature and humidity.

Table 6.1.2-1: Simulation output results

	GlobHor kWh/m2	DiffHor kWh/m2	T-Amb °C	GlobInc kWh/m2	GlobEff kWh/m2	Earray kWh	E_Grid kWh	PR
January	144.5	60.75	27.18	209.6	207	10.28	9.5	0.775
February	143.4	68.47	28.54	188.5	185.5	9.22	8.53	0.775
March	174.3	82.62	29.87	216.5	213.5	10.46	9.7	0.764
April	174.6	79.81	30.14	215	211.9	10.37	9.6	0.762
May	163.4	81.69	29.68	202	198.8	9.8	9.12	0.769
June	152.2	77.37	29.18	186.3	183.3	9.13	8.45	0.773
July	149	87.42	29.33	171.6	168.4	8.45	7.79	0.774
August	138.7	77.89	29.28	161.9	159	7.92	7.29	0.768
September	129.8	75.34	28.23	155.5	152.6	7.6	7.03	0.771
October	137.3	76.84	28.58	168.4	165.4	8.3	7.65	0.775
November	139.4	64.81	27.72	191.4	188.9	9.4	8.7	0.774
December	141.4	61.05	27.11	20.7	199.1	9.91	9.18	0.776
Year	1788	894.06	28.7367	2087.4	2233.4	110.9	102.64	0.771

where; GlobHor is the horizontal global irradiation, DifHor is th ehorizontal diffuse irradiation, T.Amb is the ambient temperature, GlobInc is the global incident in coll. plane, GlobEff is the effective global, corr, for IAM and shading, EArray is the effective energy at the output of the array, E_Grid is the energy injected into grid, and PR is performance ratio.

B 2 Table of solar tracking system result

Table B.2 indicates the experimental results for nine months, which include light intensity, environment temperature, humidity, and dual-axis solar tracking system output energy. According to table B.2, the light intensity in the months of April and May are shown to be higher than the others. This is because the polarization filter was not added in these experiment.

Table 6.1.2-2: Two-axis solar tracking output energy and environment condition

POWER	Light intensity (lx)	Humidity (%)	Temperature (°C)	Solar tracking output energy (kWh/month)
April	48102	68.5	37.11	7.801
May	38627	58.7	36.3	7.995
June	1864.3	79.18	35.4	7.25
August	1890	80.5	34.9	6.093
September	2064.1	81.2	33.24	6.422
October	3009.6	76.6	35.9	9.003
November	3383.4	75.1	34.38	10.53
December	3298.382	69.9	33.95	10.507
January	2990.73	64.5	35.7	10.53

Table 6.1.2-3: Statics panel output energy and environment condition

Month	Light intensity (lx)	Humidity (%)	Temperature (°C)	Static panel output energy (kWh/month)
April	48978.7	66.5	36.7	7.664
May	38556.3	62.8	35.4	7.64
June	1909.6	79.12	36.78	6.75
August	1876	76.5	34.9	5.7094
September	1855.5	73.92	33.8	5.714
October	2245.8	74.8	35.6	7.29
November	2611.7	66.5	34.1	9.02
December	2208.2	68.5	33.9	9
January	2317.5	65.9	36.8	9.12

BIODATA

Name – Last name: Eidi Mohammad Atif

Address: 35 Moo 5, Tumbol Klong-Nueng, Amhor Klong-Luang,

Building Bangkok Park, Pathum Thanni 12120, Thailand.

Email: ediatef@gmail.com

Contact number: +66809490219

Educational Background

: Master of Engineering in Electrical and Computer Engineering, Bangkok University, Thailand 2020

: Bachelor of Chemical Engineering, University, Jawaz Jan, Afghanistan 2012

Bangkok University

License Agreement of Dissertation/Thesis/ Report of Senior Project

Day__8 _ Month_____May____ Year___2020__

Mr./ Mrs./ Ms. Eidi Mohammad Atif now living at Bangkok Parrk, 35 Moo, 5 Street Phahonyothin Road, Sub-district Klong-Nue District Klong-Nuang Province Pathum Thani Postal Code 12120
being a Bangkok University student, student ID 7600900018
Degree level ☐ Bachelor ☑ Master ☐ Doctorate
Program M.Eng, In Electrical and Computer Engineering Department ECE Grad School Graduate School hereafter referred to as "the licensor"

Bangkok University 119 Rama 4 Road, Klong-Toey, Bangkok 10110 hereafter referred to as "the licensee"

Both parties have agreed on the following terms and conditions:

The licensor certifies that he/she is the author and possesses the exclusive rights of dissertation/thesis/report of senior project entitled Low Cost Solar Power System With Open Loop Tracking For Rural And Developing Areas submitted in partial fulfillment of the requirement for Master of Engineering in Electrical and computer Engineering of Bangkok University (hereafter referred to as "dissertation/thesis/ report of senior project").

1. The licensor grants to the licensee an indefinite and royalty free license of his/her dissertation/thesis/report of senior project to reproduce, adapt, distribute, rent out the original or copy of the manuscript.
2. In case of any dispute in the copyright of the dissertation/thesis/report of senior project between the licensor and others, or between the licensee and others, or any other inconveniences in regard to the copyright that prevent the licensee from reproducing, adapting or distributing the manuscript, the licensor agrees to indemnify the licensee against any damage incurred.

This agreement is prepared in duplicate identical wording for two copies. Both parties have read and fully understand its contents and agree to comply with the above terms and conditions. Each party shall retain one signed copy of the agreement.

_____ _____Licensor

(Eidi Mohammad Atif)

_____ _____ Licensee
(Director, Library and Learning Center)

_____Witness
(Dean, School of Engineering)

_____Witness
(Program Director)


BANGKOK UNIVERSITY
FOUNDED 1962